EUROPEAN CENTRAL BANK
EUROSYSTEM

Working Paper Series

Sulkhan Chavleishvili, Manfred Kremer, Frederik Lund-Thomsen

Quantifying financial stability trade-offs for monetary policy: a quantile VAR approach

No 2833

Abstract

We propose a novel empirical approach to inform monetary policymakers about the potential effects of policy action when facing trade-offs between financial and macroeconomic stability. We estimate a quantile vector autoregression (QVAR) for the euro area covering the real economy, monetary policy and measures of ex ante and ex post systemic risk representing financial stability. Policy implications are derived from scenario analyses where the associated costs and benefits are functions of the projected paths of the potentially asymmetric distributions of inflation and economic growth, allowing us to take a risk management perspective. One exercise considers the intertemporal financial stability trade-off in the context of the global financial crisis, where we find ex post evidence in favour of monetary policy leaning against the financial cycle. Another exercise considers the short-term financial stability trade-off when deciding the appropriate speed of monetary policy tightening to combat inflationary pressures in a fragile financial environment.

JEL Classification: C32, E37, E44, E52, G01

Keywords: Policy trade-offs, systemic risk, growth-at-risk, quantile regression.

Non-technical summary

Since the global financial crisis (GFC) of 2008-09, the debate on how monetary policy should take financial stability considerations into account has gained momentum. The controversies have centered on several related questions: First, could the GFC have been avoided if monetary policy had preemptively countered the credit boom, and what would have been the costs and benefits of doing so? Second, did the loose monetary policy stance for most of the post-crisis period have the unintended consequence of increasing financial vulnerabilities, and would economies have been better off if central banks had been less accommodative to limit financial fault lines? Finally, should central banks tighten monetary policy rapidly or gradually in response to the recent surge in inflation, with different speeds of tightening potentially implying different risks to financial stability?

This article presents an empirical nonlinear macro-financial model that is suited to quantify such important policy trade-offs. We estimate a quantile vector autoregressive model (QVAR) for the euro area on quarterly data from 1990Q1 to 2022Q4 and include measures of systemic stress and systemic vulnerabilities, consumer price inflation and real economic growth as the target variables of monetary policy makers, as well as the short-term policy rate to capture the stance of monetary policy. The QVAR presents a flexible framework that allows us to investigate the interactions between macroeconomic risks, in particular downside risks to growth and upside risks to inflation, financial stability risks and monetary policy. In addition, the nonlinear nature of the QVAR permits us to directly evaluate different monetary policy options through the lens of the central banker as a risk manager, effectively balancing the risks to the macroeconomy through policy interventions.

Through simulation exercises, we focus on two trade-offs related to financial stability which, under the right circumstances, can prove relevant to the conduct of monetary policy: The intertemporal financial stability trade-off and the intratemporal financial stability trade-off.

In the first exercise, we focus on the period prior to and during the GFC and consider a monetary policy that "leans against the wind" by hiking rates preemptively during the pre-crisis years in response to the escalating financial imbalances, and lowering them during the onset of the crisis to contain the surge in financial distress. The intuition for this type of approach is as follows: Tighter monetary policy contributes to lower leverage in the financial system by tightening financial conditions and limiting the supply of credit, thereby limiting the scale

of a potential unravelling in case of a crisis. In other words, limiting the build-up of financial vulnerabilities today, while potentially sacrificing price stability, can contribute to lower financial stability risks and consequently increase macroeconomic stability in the medium-term, which is exactly the intertemporal financial stability trade-off. Applying a risk management approach ex post, we find that such a policy would have been a net benefit, as the losses generated by the additional tightening during the pre-crisis years are outweighed by the gains stemming from a milder crisis. In the considered scenario, monetary policymakers are thus able to directly affect the intertemporal financial stability trade-off through the considered policy.

Our second exercise instead focuses on the intratemporal trade-off by considering monetary policy at the end of 2022, which was characterised by an environment of simultaneously high inflation and financial stress. In this setting, policy makers had to decide whether to hike rates rapidly, in order to avoid inflation becoming entrenched, or take a more gradual approach in service of financial stability risks. This potential dilemma encapsulates the intratemporal financial stability trade-off. Using the same risk management lens as the previous exercise favours a more gradual approach to interest rate hikes, as the balance of risks to economic activity is already tilted heavily to the downside. However, this particular conclusion, borne by the parsimonious nature of the employed QVAR, ignores some crucial points in the conduct of monetary policy pertinent to the considered scenario. First, the low and stable inflation experienced in the euro area over the estimation sample can arguably be attributed to the successful anchoring of inflation expectations at the inflation target close to 2%. Consequently, if policy makers are worried that persistently high inflation leads to a de-anchoring of inflation expectations, something not inherent in the QVAR, they may have strong preferences to bring down inflation despite the potential increase in financial stability risks. Second, policy makers have an array of tools that can be deployed for different purposes. Indeed, we model monetary policy solely through short-term interest rates, however, central banks may use other tools specifically for the purpose of containing financial stress while at the same time hiking policy rates to subdue inflation.

Still, the QVAR presented in this paper represents a flexible, nonlinear tool which, through scenario analysis, can be used to integrate the potential macroeconomic implications of financial stability risks into monetary policy geared towards achieving price stability over the medium-term.

1 Introduction

Since the global financial crisis (GFC) of 2008-09, the debate on how monetary policy should take financial stability considerations into account has gained momentum. The controversies have centered on several related questions: First, could the GFC have been avoided if monetary policy had preemptively countered the credit boom, and what would have been the costs and benefits of doing so? Second, did the loose monetary policy stance for most of the post-crisis period have the unintended consequence of increasing financial vulnerabilities, and would economies have been better off if central banks had been less accommodative to limit financial fault lines? Finally, should central banks tighten monetary policy rapidly or gradually in response to the recent surge in inflation, with different speeds of tightening potentially implying different risks to financial stability? This article presents an empirical nonlinear macro-financial model that is suited to quantify such important policy trade-offs.

Based on a parsimonious quantile vector autoregression (QVAR) model for the euro area, we investigate how financial stability conditions interact with monetary policy and its primary target variables, consumer price inflation and real GDP growth. In the model, financial stability conditions are represented by the ECB's systemic risk indicator (SRI) and the composite indicator of systemic stress (CISS). While the SRI gauges system-wide financial imbalances or vulnerabilities, the CISS quantifies the level of systemic stress in the financial system. The concepts of overall financial imbalances and systemic stress are intimately related: the first relates to systemic risk *ex ante* (i.e., the risk of a future financial crisis) and the second to systemic risk *ex post* (i.e., the severity of a realised financial crisis). A typical financial boom-bust cycle could thus be simulated by combining an elevated level of the SRI with a subsequent steep rise in the CISS, which occurs when the bubble is assumed to burst. Furthermore, since not all systemic events are ignited by the unravelling of financial imbalances like those observed prior to the GFC, including a measure of systemic financial stress as a separate variable enables us to also capture the effects of alternative sources of systemic events such as macro shocks or financial contagion (de Bandt and Hartmann (2001)). A short-term interest rate represents the setting of standard monetary policy. Estimating the model by quantile regression allows us to tease out potential nonlinearities in the macro-financial linkages, such as those highlighted in the seminal "growth-at-risk" papers by Adrian et al. (2019) and Adrian et al. (2022). In line with that literature, we find that the left tail of the economic growth distribution is much more sensitive

to systemic stress than the remaining parts of the distribution. We also detect an intertemporal relationship between systemic vulnerabilities and systemic stress, in that an increase in the former tends to precede a moderate increase in upside risks to the latter in the medium term, and that monetary policy can potentially have a direct impact on macro volatility through this intertemporal connection.

Financial stability implications for the conduct of monetary policy are derived from scenario analysis. For this purpose, we first estimate conditional forecast distributions of output growth and inflation over short- to medium-term horizons for both a baseline and an alternative policy scenario, conditional on either historical or assumed patterns of financial stability conditions. We next compute specific risk metrics from these density forecasts to help us evaluate the policy options from a risk management perspective. Within such a framework, financial stability considerations are elevated from pure "side effects" of monetary policy, to a direct channel with first-order effects on the projected paths of the distributions of inflation and output growth. The implied intertemporal balance of risks can be influenced by monetary policymakers according to their preferences over short- and medium-term gains and losses in macroeconomic stability. In order to exemplify how to quantify the different financial stability trade-offs, we perform two simulation exercises.

The first exercise runs simulations over the period 2004–2010, covering the GFC. In the baseline scenario, a set of constraints ensures that the endogenous variables follow paths that resemble the actual historical ones while still being endogenously determined. The counterfactual scenario implements a monetary policy that "leans against the wind" by increasing rates during the pre-crisis years in response to the escalation of financial imbalances, and lowering them after the onset of the crisis in response to surging financial distress. We find that such a leaning policy would have been beneficial according to risk measures that emphasise the tail risks of poor outcomes, meaning that the macroeconomic costs, ex post, of running a tighter monetary policy prior to the GFC are outbalanced by the smaller losses arising from a milder crisis.

As an alternative to this well-known *inter*temporal financial stability trade-off or "credit-bites-back" case (Kashyap and Stein (2023), Jordà et al. (2013)), the second exercise deals with an *intra*temporal or short-run financial stability trade-off. In this situation, similar to the standard Phillips-curve trade-off, policymakers must set off short-term benefits and losses in macroeconomic and financial stability against each other. We study such policy conflicts in the context of the recent surge in global inflation. In an effort to regain price stability, monetary policy

started tightening after years of ultra-low interest rates and expansionary balance-sheet policies. In doing so, central banks have to decide whether to implement tighter policies rapidly or gradually. Front-loading policy helps prevent inflation from becoming entrenched, while a gradualist approach contains risks to financial stability and economic growth stemming from disruptive financial market reactions to unusually large policy rate rises (Cavallino et al. (2022)). We run a baseline scenario from late 2022 onward, assuming that policy rates evolve according to market expectations, that commodity prices increase moderately, and that financial stress—which shot up initially along with rising inflation—abates in line with the implied model dynamics. The counterfactuals assume that interest rates rise more strongly (gradually) and to a higher (lower) level than anticipated in the baseline. The results overall support a cautious policy approach. If larger policy moves are assumed to create additional financial stress, the balance of risks tilts even further towards a more gradual course of policy action. The recent banking turmoil in the U.S. and elsewhere provide a lucid example of how monetary tightening may induce, or reveal, financial fragility (Jiang et al. (2023), Acharya et al. (2023)).

Notwithstanding the ability of monetary policy to address financial stability concerns, it is not the only game in town. The current consensus view sees macroprudential policy as the first line of defense to safeguard financial stability (Bernanke (2015)). By setting appropriate capital and liquidity buffers, for instance, macroprudential policy can counter the build-up of systemic risks and improve the resilience of the financial sector. Even so, the longer implementation lags, the limited scope and uncertain effectiveness of macroprudential policy tools leave room for monetary policy to play a complementary role in mitigating financial exuberance and stress (Freixas et al. (2015)). One of the main advantages of monetary policy is its more immediate and widespread impact on financial markets; as has been said, "*monetary policy [...] gets in all of the cracks*" (Stein (2013)).

Related literature – This paper relates to a long and broad literature on the multifaceted relationship between monetary policy and financial stability. The policy goals of financial and macroeconomic stability are seen as complementary, if not mutually conducive, in general (Freixas et al. (2015), Adrian and Liang (2016), Smets (2018)). On the one hand, financial stability is considered a necessary condition to achieve macroeconomic stability. The macroeconomic fallout from the GFC convinced academics and policymakers to upgrade their views on how costly financial crises actually are. Macro models that aim to either theoretically explain or empirically estimate the unusually large costs of financial stress on the real economy feature

nonlinearities to capture discontinuities in the macro-financial linkages brought about by, e.g., fire sale externalities, liquidity runs, and occasionally binding financial constraints. Empirically, such discontinuities reveal themselves in the heavy left-hand tails of the distribution of real economic activity conditional on measures of financial conditions (Adrian et al. (2019), Adrian et al. (2022)). On the other hand, financial stability itself depends on macroeconomic stability. This is evidenced by the surge in financial stress when the COVID-19 pandemic triggered a free fall in economic activity and dislocations in the financial sector (Chavleishvili and Kremer (2023) and Acharya et al. (2021)). As a further example, large cost-push shocks to inflation—typically accompanied by monetary tightening, an inverted yield curve and economic slowdown—tend to diminish the loss absorbing capacity and thus the resilience of financial institutions, thereby making a financial system more fragile (Jiang et al. (2023)). Finally, the inherent stability of a financial system also depends on the central bank being available, as a matter of principle, as lender of last resort to contain the risk of self-fulfilling liquidity crises (Bagehot (1873), Martin (2009)).

However, it also happens that the goals of financial stability and macroeconomic stability come into conflict. The intertemporal trade-off raised by boom-bust cycles in credit and asset prices is a prominent case in point (Schularick and Taylor (2012), Jordà et al. (2013), Jordà et al. (2015); see Boyarchenko et al. (2022) for an overview). The role of monetary policy in preventing such boom-bust cycles is two-edged, depending on the presumed causes of the boom. First, assume that the boom is driven by forces exogenous to monetary policy, such as investors' overoptimism about future profit opportunities and associated risks ("animal spirits"). The pre-crisis consensus view favoured a benign neglect approach, implying that central banks should not try to lean against the financial boom but rather clean up or mop-up the damage done to the financial system once the bubble burst. Irrational credit and asset booms were thought to be too difficult to identify in real time, and even if they were, interest rates were perceived as too blunt a tool to effectively contain the bubbles (Smets (2018)). This view seemed to be supported by the experience of the dotcom boom-bust episode in the late 1990s and early 2000s (Woodford (2012)). Supporting the sceptical stance toward the use of monetary policy to lean against the financial cycle, recent evidence also suggests that unsystematic discretionary monetary policy tightening during a financial boom may actually increase the probability of a financial crisis rather than decrease it (Schularick et al. (2021)). This notwithstanding, the GFC challenged the main assumptions underlying these views and paved the way for considering a more active

role for monetary policy in safeguarding financial stability. As noted above, systemic crises are now perceived to be much more costly than in the past (see, e.g., Gourio et al. (2018)). In addition, recent findings support the notion that policymakers may now be able to better distinguish between good and bad credit booms in real time by monitoring certain markers (see Richter et al. (2021)). Moreover, countercyclical changes in policy rates can be quite effective, especially when asset price booms are driven by leveraged short-term debt financing. Finally, it should be sufficient for policymakers to identify conditions of heightened systemic "tail risk" to justify a tighter monetary policy stance (Woodford (2012)). As a result, leaning against financial booms in order to preserve financial and macroeconomic stability beyond short-term horizons has penetrated mainstream views about optimal monetary policy strategies (Boissay et al. (2021), Woodford (2012), Goldberg et al. (2020), European Central Bank (2021)).

Second, it has also been suggested that financial imbalances can develop endogenously, in response to incentives provided by monetary policy. Indeed, Grimm et al. (2023) show that persistently accommodative monetary policy increases financial fragility and the probability of future financial distress through excessive credit and asset price growth, using more than 100 years of data for advanced economies. Freixas et al. (2015) and Kashyap and Stein (2023) summarise the theoretical and empirical literature linking risk-taking behaviour by financial institutions to the conduct of monetary policy. Central banks can induce such "reach for yield" by pursuing persistent expansionary interest rate and balance sheet policies, which have been shown to suppress risk premia on a range of financial assets (Bauer et al. (2023)). However, as the effect of monetary policy on risk premia is only temporary, the risk-taking channel is doomed to reverse, sowing the seeds of the next crisis (Kashyap and Stein (2023)). Indeed, the risk that such a "premium-bites-back" reversal could be disorderly complicates current efforts by central banks to withdraw monetary stimulus to contain inflationary pressures (Cavallino et al. (2022)). This short-term trade-off became especially apparent in September and October 2022 when the Bank of England injected fresh liquidity in government bond markets to contain systemic risks while simultaneously raising short-term policy rates to combat double digit inflation, although the ability of central banks to employ different tools to simultaneously target price and financial stability can soften the potential trade-off, as argued by (Hauser (2022)). At the strategic level, the risk-taking view also implies that monetary policy should dampen the financial cycle, but for a different reason. Countering the moral hazard stemming from central banks' lender of last resort function, monetary policy should be tighter than macroeconomic conditions would

suggest in order to limit risk-taking ex ante (Freixas et al. (2015)).

We start describing our contributions to the literature with two quotes:

> "Acceptance that monetary policy deliberations should take account of the consequences of the policy decision for financial stability will require a sustained research effort, to develop the quantitative models that will be needed as a basis for such a discussion." (Woodford (2012), p. 5)

> "How might central banks adapt their monetary-policy processes to take account explicitly of the intertemporal tradeoff we have identified? One suggestion is that policymakers should seek to develop summary measures of financial conditions that are most useful for capturing the kind of credit-bites-back risk we have highlighted." (Kashyap and Stein (2023), p. 68)

Our first contribution is to quantify the mutual dynamic relationships between two summary measures of financial stability conditions on the one hand, and inflation, economic growth and short-term interest rates, the three main variables of interest in any conventional macro model of monetary policy, on the other. Including a composite indicator of credit and asset price developments along with a systemic stress index—based on an idea put forward in Chavleishvili et al. (2021)—allows simulating all sorts of financial stability constellations and their short- and medium-run effects on inflation and growth, conditional on certain interest rate paths. The quantile VAR setup extends single-equation macro-at-risk applications into a multivariate quantile framework. By capturing the dynamic, possibly state-dependent predictive relationships between all model variables, this framework lends itself to flexible multi-period-ahead stress testing exercises as first proposed in Chavleishvili and Manganelli (2019).

Second, we present a tool that, through the use of scenario analysis, can be used to assess the short- and medium-term costs and benefits of a monetary policy that systematically takes financial stability risks into account. A strength of this "monetary policy stress-testing framework" is that it does not require an intertemporal trade-off between systemic vulnerabilities and systemic stress to be present in the estimated model coefficients.[1] Instead, any potential boom-bust cycle can be modelled through appropriate scenarios in which financial imbalances

[1]The infrequent nature of financial crises in history makes the relationship between indicators of vulnerability and the probability of future financial crises hard to estimate (Goldberg et al. (2020)). This notwithstanding, estimates for the euro area model reveal a moderate financial boom-bust relationship between the SRI and the CISS. But still, this result is not essential for our main findings.

and systemic stress are assumed to follow certain paths, representing milder or stronger financial crises. What matters is a significant impact of systemic stress on the short-term outlook for real growth as well as some leverage of monetary policy on financial and macroeconomic conditions. Since the short-term predictive power of financial conditions for economic growth appears to hold across countries, our framework should also work for economies where no major financial crisis occurred over the estimation period.

Third, we suggest an intratemporal financial stability trade-off for monetary policy, which is particularly acute when monetary policy needs to tighten—through interest rate and/or quantitative policies—in the face of adverse shocks to inflation. In such circumstances, policy-induced financial stress can magnify the usual Phillips-curve trade-off. In this context, our model can be seen as an empirical counterpart to the theoretical model of Stein and Sunderam (2018) on monetary policy gradualism when central banks care for bond market volatility. The CISS includes measures of bond, equity and foreign exchange market volatility, apart from risk premia and other valuation indicators, thus allowing for a more general perspective on financial market discontinuities disliked by policymakers (Coibion and Gorodnichenko (2012)).

Fourth, we show how the QVAR can be used to operationalise a monetary policy risk management framework (Kilian and Manganelli (2008)) that systematically incorporates financial stability considerations with the aim of balancing short- to medium-term macroeconomic risks. This risk management perspective offers an alternative to existing frameworks to study the costs and benefits of leaning against the wind policies (see Svensson (2017), Brandao-Marques et al. (2020), Filardo and Rungcharoenkitkul (2016)). Finally, the paper also makes a modest methodological contribution by proposing a Shapley value decomposition to identify the driving factors of the model forecasts for any variable and any specific quantile of interest.

The paper is structured as follows. Section 2 introduces the lens with which we perceive financial stability risks along different dimensions. Section 3 presents the QVAR framework and how to apply it in scenario analyses, while section 4 specifies the QVAR model and describes the data. Section 5 estimates the model and dissects the inherent model dynamics and nonlinearities. Sections 6 and 7 present the scenarios for the intertemporal and intratemporal financial stability trade-offs, respectively. Section 8 concludes.

Figure 1: Time series of the euro area CISS and SRI, 1990Q2:2022Q4

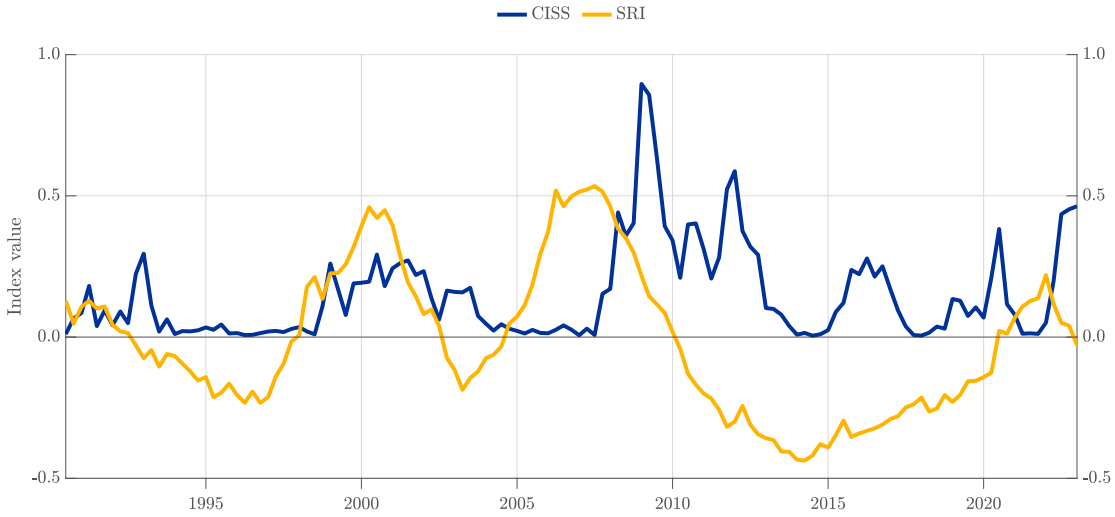

Source: ECB.
Note: The CISS is constructed to take values between $[0; 1]$.

2 Operationalising financial stability

To motivate the financial stability trade-offs for monetary policy, we begin by considering financial stability as broadly spanning two related but distinct dimensions, systemic vulnerabilities and systemic stress. Systemic vulnerabilities reflect the built-up yet docile risk of systemic nature within a financial system, some or all of which materialises at a future point in time with some probability. Systemic stress, on the other hand, is the realisation of all or part of said risk.

To illustrate the complementary nature of financial vulnerabilities and stress in the euro area, figure 1 depicts prevailing stress in financial markets, as captured by the composite indicator of systemic stress, CISS (see Hollo et al. (2012), and Chavleishvili and Kremer (2023)), and cyclical systemic vulnerabilities stemming from economic and financial imbalances, reflected in the systemic risk indicator, SRI (see Lang et al. (2019)). Prolonged periods of elevated levels of the CISS are seen to be regularly, though not always, preceded by a persistent increase in the SRI, capturing the build-up of vulnerabilities in the financial system, after which the SRI declines in response to the heightened volatility.[2] Unsurprisingly, the GFC in 2008 and 2009 is the most notable example of this intertemporal relationship, representing a tail event in which

[2]The surge in the SRI in 2020Q2 is in large part a result of the sharp decline in real GDP growth experienced during the COVID-19 pandemic, which mechanically caused select sub components and consequently the SRI itself to increase.

a large share of the pent up vulnerabilities materialised.

The pattern above is not coincidental. Indeed, the SRI belongs to a broad class of early warning-indicators built with the express purpose of flagging widening financial imbalances of systemic nature (e.g. Alessi and Detken (2018)). In particular, the SRI combines several sub-indicators representative of different categories relevant for gauging trends in systemic risks, most notably linked to 2 to 3-year changes in real asset prices and credit.[3] Having both asset price and credit measures makes the SRI well suited to study the interaction between systemic risks ex ante and ex post, as Jordà et al. (2015) show that asset price bubbles driven by credit booms can lead to particularly detrimental outcomes for the real economy. Further, the use of multi-year changes in the underlying indicators implies that the SRI represents cycles of a more persistent nature, thus contributing to its slow-moving nature by filtering out long-run trends as well as short-run fluctuations (see Hamilton (2018)).[4]

The observed co-movement between systemic vulnerabilities and stress motivates the general notion of a potential intertemporal financial stability trade-off for monetary policy. While accommodative monetary policy tends to reduce financial stress and macroeconomic volatility in the short term, it may also encourage the build-up of financial imbalances over the medium term, thereby increasing the likelihood of heightened financial stress and macroeconomic instability over longer horizons. This is intuitive, as periods of tranquility, characterised by low uncertainty and ample financing opportunities, may increase risk-taking and, consequently, leverage in the financial system. Conversely, by tightening monetary policy, central banks can provide incentives for private agents to unwind risky financial positions and deleverage, thereby reducing the likelihood of financial distress in the future at the cost of increased financial and macroeconomic instability today.

Figure 1 shows that financial distress can also arise due to macro shocks and financial contagion, unrelated to the prior accumulation of systemic vulnerabilities. For instance, the war in Ukraine which started in early 2022 brought about a surge in systemic stress, partly related to the global bout of inflation following the huge increases in the energy and food prices, among

[3]The SRI is a weighted-average of the following components: two-year change in the bank credit-to-GDP ratio; two-year growth rate of real total credit; two-year change in the debt-service-ratio; three-year change in the residential-real-estate price-to-income ratio; three-year growth rate of real equity prices; current account-to-GDP ratio.

[4]Notably, Lang et al. (2019) show that the SRI performs equally well as an early warning indicator for financial crises when only using data prior to 2000Q1, supporting its signalling value outside of the period leading up to the GFC.

others. Another example is the spreading risk of contagion from the downturn of the large hedge fund Long-Term Capital Management in 1998.

3 QVAR framework

3.1 The QVAR model

The QVAR combines the methods of structural vector autoregressions and quantile regressions (Koenker and Bassett Jr (1978)), as laid out in more detail by Chavleishvili and Manganelli (2019).

Specifically, letting $j \in (0;1)$ be an index of quantiles to be estimated, the QVAR can be formalised as

$$Y_t = C^j D_t + A_0^j Y_t + \sum_{p=1}^{P} A_p^j Y_{t-p} + \sum_{s=0}^{S} B_s^j X_{t-s} + \varepsilon_t^j \tag{1}$$

$$F\left(\varepsilon_{i,t}^j < 0 | \Psi_{i,t-1}\right) = j \; \forall \, i = 1, 2, \ldots, K \tag{2}$$

where Y_t is a $K \times 1$ vector containing the endogenous variables at time t, X_t an $M \times 1$ vector containing the exogenous variables, D_t an $R \times 1$ vector of deterministic terms, ε_t^j the error term at quantile j and $\{C^j, A_0^j, A_1^j, \ldots, A_P^j, B_0^j, \ldots, B_S^j\}$ a set of coefficient matrices for quantile j, with A_0^j in particular being lower triangular and having a zero diagonal. The design of A_0^j is what grants the model its structural quality, in particular through a Cholesky decomposition common in the structural VAR literature (e.g. Christiano et al. (1999)). Equation (2) is the identifying assumption used in quantile regressions. It provides that for an unspecified cumulative distribution function, $F(\cdot)$, the jth quantile of variable i's quantile error, $\varepsilon_{i,t}^j$, equals 0 conditional on the information set $\Psi_{i,t-1}$, containing realisations of lagged values of Y and X as well as contemporaneous values of X and y_k for $k = 1, ..., i$.

The inclusion of X_t in equation (1) is a special case of Chavleishvili and Manganelli (2019), in which a set of variables assumed strictly exogenous, meaning there is no feedback from Y_t into X_t or between any individual variable in X_t. The choice of X_t and the associated exogeneity assumptions are discussed in greater detail in section 4.

3.2 Conditional quantile forecasting and scenario analysis

The QVAR given by equations (1)-(2) jointly models the quantile forecasts of the endogenous variables conditional on their past realisations, and using the simulation methods detailed in Koenker et al. (2017) and Chavleishvili and Manganelli (2019), the model can be used to forecast the conditional joint distribution of the system. A more thorough description on conditional quantile forecasting with the QVAR is given in appendix B, and we refer the reader to this appendix as well as the literature above for more details on the methodology as well as the simulation algorithm employed. However, we briefly describe the general idea here to provide some intuition. Importantly, we project the conditional distribution of individual exogenous variables forward using a univariate version of the approach described below, although other approaches, including those not based on regression quantiles, could be employed.[5] For this purpose, it can be instructive to think of the QVAR as a random coefficient model (Koenker and Xiao (2006) and Chavleishvili and Manganelli (2019)). Consider then again equation (1), dropping exogenous terms without loss of generality, but rewritten in the random coefficients representation

$$Y_t = C\left(U_t\right) D_t + \sum_{p=0}^{P} A_p\left(U_t\right) Y_{t-p} \tag{3}$$

where the matrices of parameters in C and $A_\bullet$ are now determined by the i.i.d. standard uniform variable, U_t, with support $(0;1)^K$, which maps into a set of estimated quantile coefficients. From equation (3) it becomes clear that the forward motion of the entire system up to horizon H from period τ can be forecast by selecting a set, $\{U_{\tau+h}\}_{h=1}^{H}$, which will then determine the parameters governing the endogenous variables at each point in time. This set can either be chosen directly by the researcher or drawn randomly. The simulation approach listed above takes the latter approach, and by estimating the model (1)-(2) for a sufficiently granular set of quantiles, η, a random draw of $U_{\tau+h}$ can subsequently be mapped to a particular selection of quantiles, $\lambda_{\tau+h} \in \eta$, one for each endogenous variable, which then dictates the behaviour of $Y_{\tau+h}$ as given by (3). Repeating the conditional forecast a sufficient number of times then yields the complete joint forecast distribution of the system at each point in the forecast horizon.

Once the method for producing conditional quantile forecasts is in place, scenario analysis

[5] As such, we could equivalently model the exogenous variables as endogenous with an appropriate set of zero restrictions on the relevant coefficients.

follows naturally through an appropriate set of restrictions on the model. We once again refer the reader to appendix B for more details on how to do scenario analysis in the QVAR and provide a brief description here.

One way to do simple scenario analysis in the QVAR is by imposing a series of shocks throughout the forecast horizon, for instance a set of monetary policy shocks or inflationary shocks. A special case of scenario analysis with structural shocks is when the shocks are chosen such that one or more of the endogenous variables realise a specific path (see e.g. Leeper and Zha (2003) and Giannone et al. (2019)). This can be useful if, for instance, one wants to investigate how a specific interest rate path would affect the predictions of the model. One major difference between this type of analysis in the the QVAR and linear VARs is that shocking the latter implies a shock to the mean of the forecast distribution, consequently shifting the entire distribution in the direction of the shock, while it is in principle possible to impose different shocks on different quantiles in the QVAR. Shocking the different quantiles in a non-symmetric way increases the complexity of the exercise substantially, however, and for our purposes we therefore only consider shocks to variables that are equal across the forecast distribution.

Particular to the QVAR, another way to do scenario analysis is to restrict the realisations of $U_{\tau+h}$ throughout the forecast horizon. Instead of randomly picking a quantile when simulating the QVAR forward, we can also select a specific path of the $U_{\tau+h}$ which fixes the parameters governing the model dynamics in a given period. In this way, the QVAR allows for the endogenous variables to be pushed along a desired path through the choice of $U_{\tau+h}$ while still being endogenously determined, allowing for counterfactual analysis over historical episodes, as we will demonstrate below.

4 Model specification

4.1 Endogenous variables

Our set of endogenous variables consists of the CISS and SRI to capture realised systemic risk and systemic vulnerabilities, log-differences of harmonised consumer prices and euro area real GDP representing the real economy as well as the changes in the 3-month EUR overnight index swap (OIS) rate as a measure of standard monetary policy.[6] We include two lags of Y in our

[6]Supporting the inclusion of the SRI and 3-month OIS rate, a variable selection exercise considering model fit (see Lee et al. (2014) and Machado (1993)) and forecasting ability finds that these particular variables perform relatively well vis-à-vis other measures of financial imbalances and monetary instruments.

model as a compromise between the need to appropriately capture relevant model dynamics and the typical issue of dimensionality in VARs with limited sample size, see also section 4.3.

As noted previously, the applied QVAR imposes a recursive identification scheme to identify the structural model, and we order the block of real economy variables, i.e. real GDP growth and consumer price inflation, before monetary policy instruments, in our case the 3-month EUR OIS rate, similar to e.g. Christiano et al. (1999). The structural implication is that monetary policy can respond to macroeconomic developments within the current period, while real economic activity only responds to monetary policy with a delay. The notion of monetary policy transmission lags is well documented in the literature (Havranek and Rusnak (2013)) making this particular ordering a natural choice. Additionally, we impose an implementation lag of monetary policy on the real economy, akin to Estrella (2015), by requiring that the first lag of changes in the 3-month OIS rate impacts neither economic activity nor inflation directly, but only implicitly through the financial block. Specifically, we estimate the model setting the elements corresponding to the 3-month OIS rate in $A^j_{1,HICP}$ and $A^j_{1,GDP}$ equal to 0 for all j.

Second, we place the financial stability block, that is, the CISS and SRI, before real economy and monetary policy variables. This choice in large part reflects the desired model property of allowing severe shocks originating from the financial system to affect the macroeconomy "instantaneously", i.e. within the data sampling period. The most prominent example of this type of dynamic was seen during the GFC, where increased risk aversion and uncertainty about the solidity of the financial sector, though not necessarily about the macroeconomy at the outset, led to a self propagating evaporation of liquidity in interbank and other key funding markets, evolving into a full blown liquidity crisis with severe and immediate consequences for economic activity (Borio (2010)).[7] [8]

[7] However, placing the financial stability block first in our structural identification is largely an inconsequential choice, as a reverse ordering leads to similar results.

[8] One may also consider the placement of the CISS as reflecting an information lag as suggested in Inoue et al. (2009). While financial asset prices can be observed more or less in real time, economic agents receive information about current GDP and inflation with a lag of several weeks. Accordingly, it may be assumed that the CISS - being composed of readily observable asset prices - can influence financial and real quantities contemporaneously, while the opposite may not necessarily apply since credit volumes, real GDP as well as housing and consumer prices are published only with significant delays and are thus not known to agents when taking financial and economic decisions in time t.

4.2 Exogenous variables

In order to capture supply side pressures of more global origin, we include commodity price inflation based on the S&P GSCI index, which reflects price movements in global commodity markets, as our only exogenous variable with two lags. The addition of commodity prices serves two purposes: The macroeconomic environment following the COVID-19 pandemic in 2020 put the spotlight back on the pass-through of supply side factors into consumer prices, which had remained relatively benign for the previous decade. Hence, commodity prices help expand the dimensions of the QVAR pertaining to supply side dynamics. Second, commodity prices are often identified as alleviating the "price puzzle" often present in VARs, see e.g. Sims (1992) and Sims and Zha (2006).

The assumption of commodity prices as exogenous is not necessarily innocuous since they are determined by global supply and demand (Kilian (2009)), the latter of which the euro area constitutes a non-negligible share of. To this point, oil prices, which make up almost half of the S&P GSCI index, are generally recognised as hard to predict with standard statistical models (Hamilton (2009)), and it is therefore often assumed that they evolve exogenously to individual economies (see also Kilian and Vega (2011) and Kilian and Vigfusson (2013)). We support the assumption of exogeneity of commodity prices by running a range of block exclusion tests on our model variables which fail to reject the null hypothesis of no direct predictive power of the euro area macro variables on commodity prices.

To allow us to identify commodity price shocks as supply shocks, we restrict our model in (1)-(2) such that structural effects of commodity prices on the system of endogenous variables only enter through consumer price inflation, i.e. the coefficients of $B^j_{s,i\neq HICP}$ associated with commodity price inflation are set equal to zero for all j, i, s. Without this particular restriction, model estimates will tend to conflate global supply and demand shocks within commodity prices, thereby weakening the case for identifying the associated shocks as supply shocks.

4.3 Data

We estimate the QVAR on quarterly data over the period 1990Q1-2022Q4, totaling 132 observations. Quarterly values of the CISS are computed as quarterly averages of daily values, while consumer and commodity price inflation are the log-difference in the quarterly average of the seasonally adjusted HICP and commodity price index, respectively, at a monthly frequency. We

use the change in quarterly averages for the 3-month OIS rate as the monetary policy instrument.

The inclusion of the COVID-19 outbreak and its subsequent effects in the sample necessitates a careful approach to the exact specification of the QVAR, as the extraordinary movements in real GDP growth can severely interfere with estimation coefficients (see also Lenza and Primiceri (2022)). Indeed, estimating the QVAR for the entire sample without any regard for the COVID-19 shock results in notably stronger mean reversion for real GDP growth, in particular when compared to a model estimated on data ending in 2019Q4. We account for the pandemic by adding a set of dummy variables (D_{2020Q1}, D_{2020Q2}, D_{2020Q3} and D_{2020Q4}), one for each quarter in 2020. Although this approach increases the dimensionality of the model, they ensure that the effects of the COVID observations on estimated coefficients remain relatively muted. In addition to the four dummy variables, we include a constant term. In contrast to the COVID-19 crisis, we do not include dummies for the GFC. While the nonlinear interactions between the financial and the macroeconomic variables during the GFC are well captured by the QVAR, the COVID-19 crisis produces extremely oversized model residuals of the real variables far from the tails of the prior historical distributions if not accounted for explicitly.

Euro area macroeconomic data prior to 1999 stems from the Area Wide Model developed by Fagan et al. (2005). The Area Wide Model synthesises several country-level data series to create a new set of time series reflecting euro area aggregates, had the currency union existed before 1999.[9]

Like aggregate euro area data, EUR OIS markets were not sufficiently active or liquid to construct OIS rates until the beginning of 2000. As such, we approximate the 3-month OIS rate before 2000 by using the backcasted 3-month EURIBOR rate from 1994Q1-1999Q4 corrected for the average spread to the EUR OIS rate in the period 2000Q1-2007Q2. Before 1994 we use the 3-month FIBOR rate, the German interbank rate, corrected for the same average EURIBOR-OIS spread as above as well as the average spread between FIBOR and EURIBOR at the 3-month tenor from 1994Q1-1998Q4.

Time series for endogenous and exogenous variables are plotted in appendix A with the exception of the CISS and SRI, which are separately illustrated in figure 1.

[9]The data set is made publicly available by the Euro Area Business Cycle Network.

5 Nonlinearity and model dynamics

We estimate the QVAR specified above and confirm its nonlinearity through Wald tests of the equality of slopes across quantiles, see Koenker (2005). Specifically, we test the null hypothesis that the slope parameters are equal to the median estimates across quantiles, that is, $A_{0,i}^{j\neq 0.5} = A_{0,i}^{0.5}$, $A_{p,i}^{j\neq 0.5} = A_{p,i}^{0.5}$ and $B_{s,i}^{j\neq 0.5} = B_{s,i}^{0.5}$. Failure to reject the null indicates that there is no nonlinearity in the direct predictive power of one variable on another. We perform the test for each endogenous variable by individually estimating the quantile equations across deciles in the interval $[0.1; 0.9]$ and compute the Wald test statistic. The test follows a χ^2-distribution where the degrees of freedom equal the number of slope parameters we wish to test, i.e. the number of non-zero restricted coefficients in $A_{0,i}^{j}$, $A_{p,i}^{j}$ and $B_{s,i}^{j}$, times the total number of estimated quantiles, not counting the median, which we test against, in this case 8. Consequently, the degrees of freedom will vary depending on the ordering in the structural identification and the number of additional zero restrictions imposed, as discussed in the previous section. The results of the Wald tests are reported in table 1. The test rejects the null of slope homogeneity for all endogenous variables except HICP inflation and the SRI, but only marginally for the latter.

Table 1: Wald tests of parameter homogeneity

	Test statistic	DF	p-value
$CISS$	116.87	80	0.00
SRI	109.99	88	0.06
$\Delta ln(HICP)$	111.31	112	0.50
$\Delta ln(GDP)$	145.41	96	0.00
$\Delta OIS_{3M}^{€}$	316.51	112	0.00

Source: Authors' calculations.
Note: Test statistics are calculated individually for each endogenous variable and for each decile in the closed interval $[0.1; 0.9]$. P-values are based on a χ^2-distribution.

The estimated nonlinearities are also present in the generalised quantile impulse response functions (G-QIRFs). The G-QIRFs are computed following Chavleishvili and Mönch (2023) using the simulation approach described in appendix B.[10] The entire set of G-QIRFs can be found in figures A.5 and A.6 in appendix A. The remainder of this section highlights some G-QIRFs that are particularly relevant in our context.

[10] We compute bootstrapped confidence intervals for the G-QIRFs based on the moving block bootstrap procedure (see Fitzenberger (1998) and Härdle et al. (2003)).

Figure 2: Impact of a CISS-shock on select quantiles of real GDP growth and the SRI

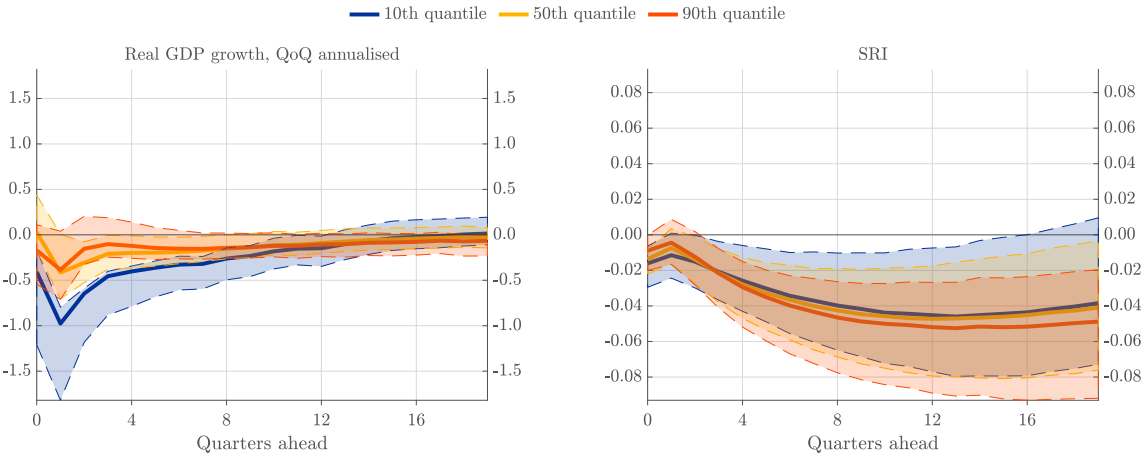

Source: Authors' calculations.
Note: G-QIRFs for the SRI (right) and real GDP growth (left) of a shock to the CISS based on 10^6 forward simulations. The shock equals the standard deviation of the errors in the CISS-equation at the 50th percentile. Initial conditions are set equal to the historical median values of the respective time series. Shaded areas indicate bootstrapped 90% confidence intervals using $5,000$ bootstrap iterations with 2×10^4 forward simulations each.

5.1 Effects of macro-financial shocks

The quantile-specific dynamic multipliers plotted in the right-hand panels of figures 2 and 3 reveal mutual dependence between our two dimensions of financial stability. To help interpret those impulse responses, we also plot the corresponding responses of real GDP growth in the left-hand panels of figures 2 and 3. First, a positive shock in the CISS correlates with a prolonged, significant decline in the SRI, which is rather homogeneous across quantiles. This pattern confirms our expectations that a surge in financial stress tends to gradually depress financial activity and asset prices. However, there is a notable asymmetry in the reaction of real GDP growth to a CISS shock. In particular, an increases in the CISS predicts a much stronger drop in real economic activity in the lower tail of the growth distribution, and the differences between the QIRF at the 10% quantile and those at the median and the 90% level are also statistically significant. This overall pattern may suggest that the frictions associated with financial stress produce highly nonlinear contractions in economic activity mainly during bad states of the world.

Second, a positive shock to the SRI is associated with a rapid decline in the CISS which is stronger, and statistically significant, in the right tail of the CISS distribution. One possible interpretation of this comovement is that the increase in the SRI reflects an easing of financial

Figure 3: Impact of an SRI-shock on select quantiles of real GDP growth and the CISS

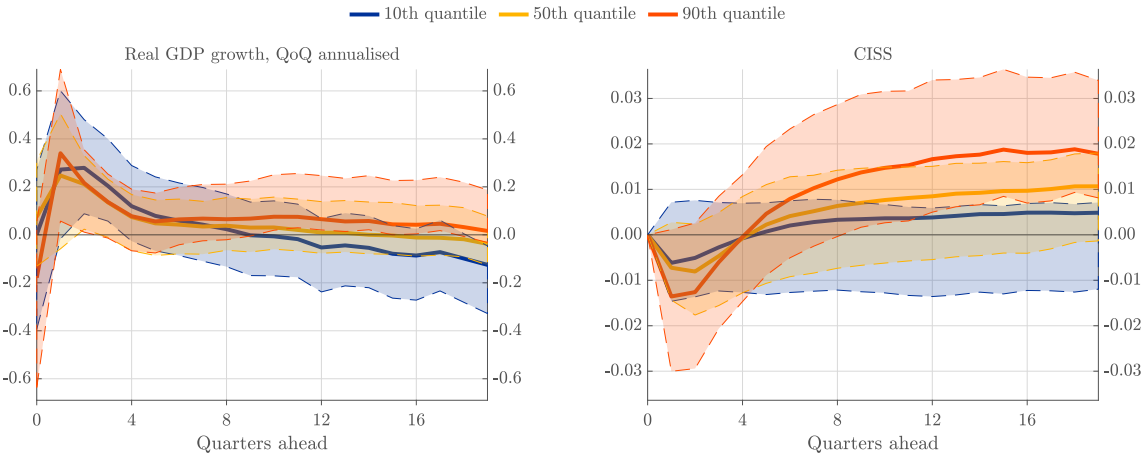

Source: Authors' calculations.
Note: G-QIRFs for the CISS (right) and real GDP growth (left) of a shock to the SRI based on 10^6 forward simulations. The shock equals the standard deviation of the errors in the SRI-equation at the 50th percentile. Initial conditions are set equal to the historical median values of the respective time series. Shaded areas indicate bootstrapped 90% confidence intervals using $5,000$ bootstrap iterations with 2×10^4 forward simulations each.

constraints and greater risk-taking in the system, implying stronger economic activity and lower risk premia and market uncertainty. However, this dampening effect on financial stress tends to reverse over the medium term, as indicated by the significant reversal in the upper conditional quantile of the CISS at the 2-3 year horizon. Switching the sign of the assumed SRI shock, the strong initial reaction of the CISS in the upper tail of its distribution may also point to a temporary vicious circle between financial activity and stress during crisis episodes.

5.2 Effects of monetary policy

In what follows, we interpret changes in the short-term interest rate as being driven by monetary policy. The top row of figure 4 plots the responses of the conditional distributions of inflation and real GDP growth to a positive interest rate shock. As expected, monetary policy shocks in the QVAR are associated with deflationary and contractionary outcomes for the real economy. The effects of an interest rate shock on economic activity are rather rapid and clearly statistically significant across all quantiles shown. The effects die out after about a year. The effects on inflation, on the other hand, are delayed by several months, are basically linear, as seen by the symmetric response of the different quantiles, and become statistically significant only in the upper tail of the conditional distribution. The persistent nature of the effects may reflect the

near-unit root in the inflation process over our sample of data. [11]

Figure 4: Impact of an interest rate shock on select quantiles of the real and financial blocks

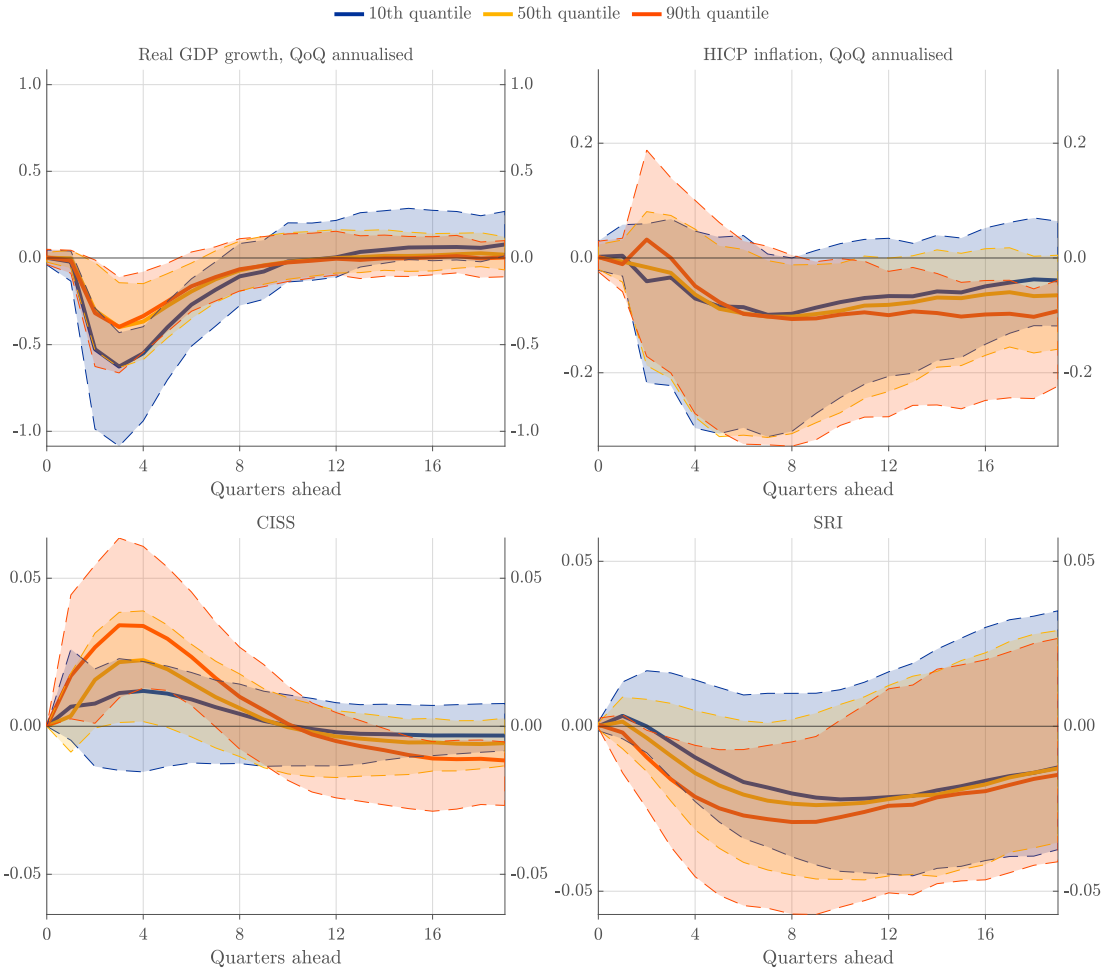

Source: Authors' calculations.
Note: G-QIRFs for real GDP growth (top left), HICP inflation (top right), QoQ annualised values, CISS (bottom left) and the SRI (bottom right) of a shock to interest rates based on 10^6 forward simulations. The shock equals the standard deviation of the errors in the interest rate equation at the 50th percentile. Initial conditions are set equal to the historical median values of the respective time series. Shaded areas indicate bootstrapped 90% confidence intervals using $5,000$ bootstrap iterations with 2×10^4 forward simulations each.

The financial stability trade-offs of monetary policy require a link between the policy instrument and our macro-financial variables capturing systemic risk. The bottom row of figure 4 plots the response of the CISS and SRI to changes in interest rate. Indeed, we see that a positive interest rate shock leads to an upward shift in the conditional forecast distribution of

[11] The impact of the short-term interest rate on inflation estimated in the QVAR imply elasticities similar to those found by Rusnák et al. (2013), while the larger initial impact on output is a common occurrence in the structural VAR literature, e.g. Mojon and Peersman (2001).

the CISS, with upside risks in particular becoming gradually stronger and significant over time. Financial vulnerabilities, on the other hand, tend to become persistently lower following a tighter monetary policy stance, potentially capturing the higher interest rates permeating through the system, tightening financial conditions as a result, significantly so for the lower quantiles.

The properties of the estimated macro-financial linkages, including those assumed to reflect monetary policy, principally support the existence of the two financial stability trade-offs in the euro area. Specifically, tightening monetary policy today may alleviate the build-up of financial imbalances, entail short-term losses in economic output, but bring about positive effects on macroeconomic stability in the medium term. Likewise, increased inflationary pressures, particularly when driven by supply-shocks, requires policymakers to raise interest rates, even if tighter monetary policy generates a near-term increase in systemic stress and downside risks to growth.

6 Leaning against the financial cycle with monetary policy

In order to highlight the role of monetary policy in different macro-financial states, we now use the QVAR to analyse a scenario characterised by a credit-fuelled economic boom and bust, modelled after the GFC and the period leading up to it. In this scenario, the central bank is faced with the intertemporal financial stability trade-off as it can effectively reduce expected losses in the medium term by adjusting its policy, although at the cost of allowing price instability in the short term. In the next section, we will instead consider a scenario highlighting the intratemporal trade-off.

6.1 Calibration

When engineering a financial crisis in the QVAR with the intent of performing counterfactual policy analysis through conditional forecasting, it is important that the financial and real economy variables are allowed to respond to changes in monetary conditions both before, during and after the crisis. Hence, the implementation method discussed in section 3 is not a trivial one.

To begin with, we choose 2004Q3 as our forecast origin as this point marked the beginning of an accelerating increase in systemic vulnerabilities that eventually culminated in the GFC (figure 1), making it a suitable starting point for counterfactual analysis.

In order to replicate the initial build-up and subsequent unraveling of financial vulnerabilities,

Table 2: Conditional percentile realisations for the CISS, SRI, inflation and real GDP growth

	2004	2005				2006				2007				2008			
	Q4	Q1	Q2	Q3	Q4	Q1	Q2	Q3	Q4	Q1	Q2	Q3	Q4	Q1	Q2	Q3	Q4
CISS	30	30	35	45	40	30	30	30	20	20	20	85	45	95	30	90	95
SRI	45	80	90	90	90	90	30	60	60	60	60	50	25	25	-	-	-
HICP	-	-	-	-	-	-	-	-	-	-	-	-	-	-	-	-	-
GDP	-	-	-	-	-	-	-	-	-	-	-	-	-	-	-	10	10

Note: A hyphen ('-') indicates the absence of any quantile restriction.

we impose quantile paths on the SRI, CISS and real GDP growth to mimic the realised values over the restricted periods (table 2).[12] In this way, we take advantage of having endogenously modelled the entire conditional forecast distribution, allowing us to consider how monetary policy changes the shape and location of the conditional distributions of the endogenous variables, both directly and indirectly.

Note that the assumed paths of the SRI and the CISS imply a financial boom-bust cycle as it actually occurred in the GFC. However, we could have also assumed that the GFC never happened, and that the SRI mean-reverted in a smooth fashion. The design of a financial stability scenario does not depend on the presence of an intertemporal relationship between our measures of ex ante and ex post financial stability risks in the QVAR coefficients. Instead, any a priori information outside the model can be used to impose certain paths for financial imbalances and financial stress through an appropriate choice of restrictions. What matters for a financial stability trade-off to exist is a significant impact of systemic stress on the short-term outlook for real growth as well as some leverage of monetary policy on financial and macroeconomic conditions.[13]

In the baseline scenario, policy rates are fixed to their observed values over the simulation horizon, assuming no uncertainty equivalent to a collapse in the conditional distribution, as discussed in appendix B. Commodity prices follow a univariate quantile AR process as described earlier. The counterfactual scenario considers an alternative path for monetary policy guided by "leaning against the wind" considerations (see figure 5). In this alternative policy scenario, rates respond counter-cyclically to the financial cycle, rising more during the boom (preemptive

[12]The select restrictions on growth ensure a more accurate reflection of realised values in the exercise and do not affect the qualitative results.

[13]For instance, Chavleishvili et al. (2021) uses an QVAR to directly model how stabilising the financial cycle affects real GDP growth in a financial stress event, even though their model does not explicitly find an intertemporal link from the financial cycle to financial stress.

Figure 5: Path of the 3-month EUR OIS rate before and during the GFC in the baseline and counterfactual scenario

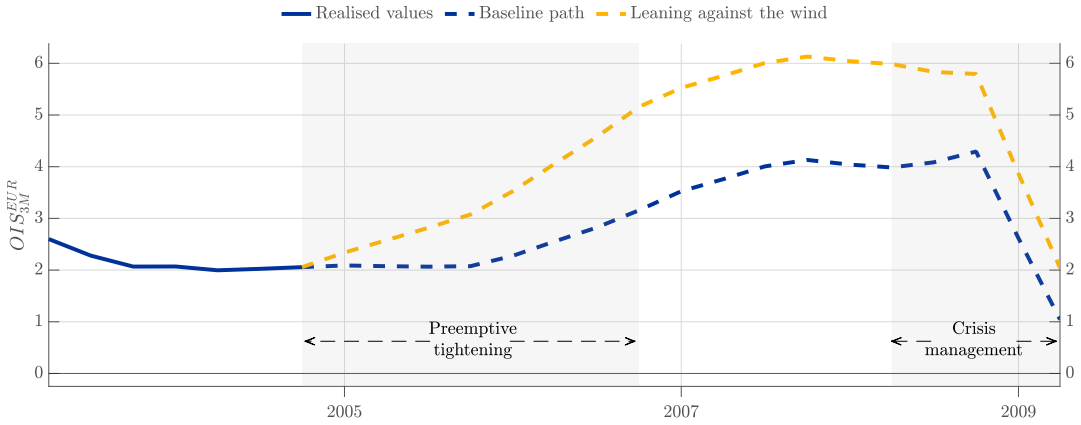

Source: ECB and authors' calculations.

tightening) and declining more during the bust (crisis management) (discussed in, e.g., European Central Bank (2021)). Specifically, we assume that policy rates are increased by an additional 25 basis points each quarter in the period 2004Q4:2006Q3, totaling two percentage points, and lowered by 25 basis points extra for four consecutive quarters at the onset of the crisis in 2008Q1.

6.2 Results

Figure 6 shows the conditional quantile forecasts of the macro-financial variables in the baseline and counterfactual scenario described above. The chart also includes realised values for reference. The bands depicted in figure 6 should not be interpreted as conventional confidence bands, as they hold no direct information about statistical significance or forecast error. Rather, they are point predictions of select, separately modeled quantiles from the conditional forecast distribution of the endogenous variables, each accompanied by their own statistical uncertainty which we do not report here. In a correctly specified model, we should consequently expect to observe 10 percent of realised values below the 10th quantile, 25 percent below the 25th quantile and so forth, as per the standard quantile definition. Showing the time profiles of conditional tail risks is the conceptual essence of macro-at-risk frameworks. Several things are worth noting.

First, the baseline scenario for output and inflation (blue in the charts) reasonably captures the actual time series observed up until 2008Q4. In particular, both the conditional forecasts for GDP growth, where barely any restrictions are imposed, experience a financially driven boom, bust and subsequent recovery remarkably similar to the de facto historical patterns.

Figure 6: Conditional quantile forecasts of the real and financial variables over the financial boom and bust in the baseline and counterfactual scenarios

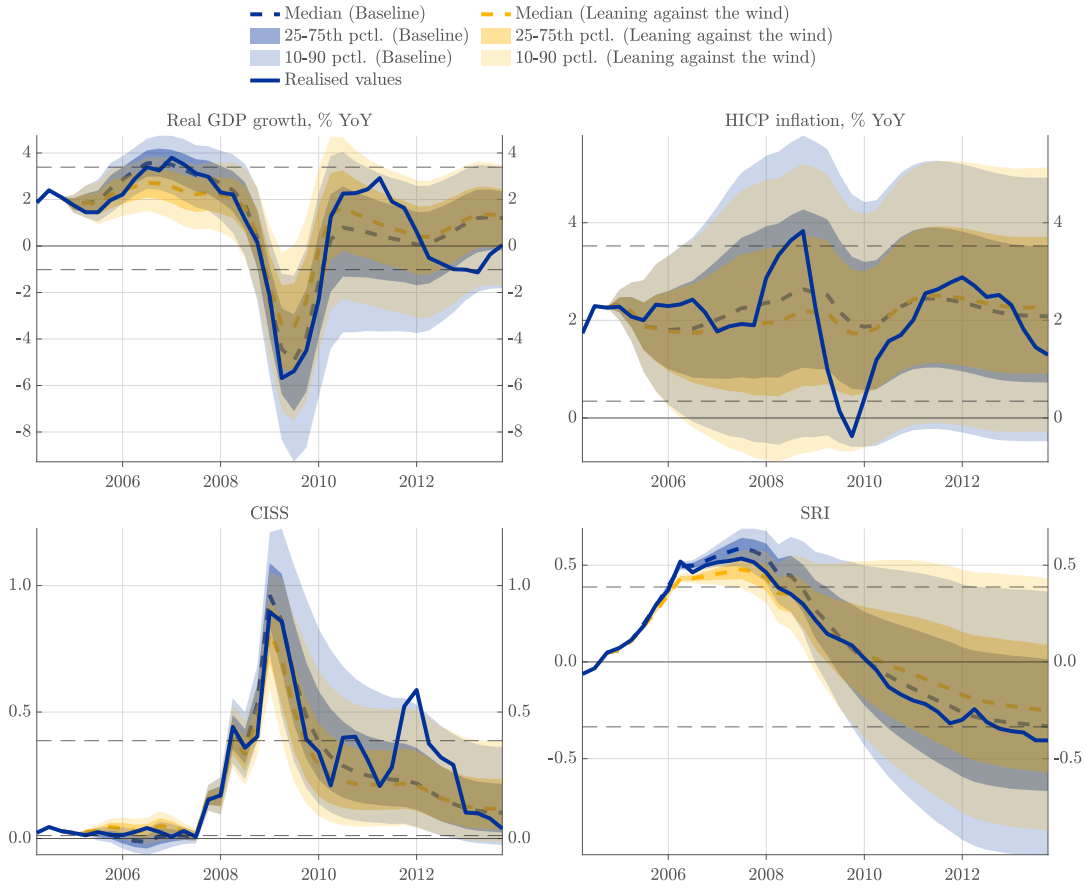

Source: ECB and authors' calculations.
Note: Based on 10^6 forward simulations using 2004Q3 as forecast origin. Horizontal dashed lines indicate the 10th and 90th unconditional percentiles, respectively.

Additionally, the conditional growth distribution is more negatively skewed in contrast to the more symmetric inflation distribution, in line with the estimated model dynamics.

Second, by leaning against the financial cycle (yellow in the charts), monetary policy would curb the build-up of systemic vulnerabilities ahead of the GFC. This is seen by the counterfactual forecast distribution of the SRI peaking at around 0.45, compared to 0.60 in the baseline. As a result, the subsequent sudden materialisation of systemic stress would be more subdued in the counterfactual scenario, cushioning the systemic deleveraging taking place during the crisis, and in turn lowering downside risks to growth substantially.

Third, preemptive action by monetary policy is not without cost. As can be seen from the figure, the conditional forecast distribution of real GDP growth is shifted downward in the pre-

crisis period by 1-2 percentage points. The inflation forecast distribution is also shifted downward over the pre-crisis period, with median inflation dropping well below the ECB's "below but close to 2%" inflation aim at that time. However, these losses in growth and inflation stabilisation in the counterfactual scenario have to be offset against the smaller drop in growth and inflation during the height of the crisis. We address these trade-offs more systematically at the end of this section.

To explore the main driving forces of how monetary policy "leaning" influences financial stability and economic conditions in more detail, we perform a Shapley value decomposition of the quantile projections in the baseline and counterfactual scenarios. The suggested Shapley value decomposition dissects the projected conditional quantile paths of any endogenous model variable in both the baseline and the counterfactual scenarios into contributions from each included model feature.[14] Shapley values represent a convenient tool for 'model explainability' and forecast performance evaluation in highly nonlinear model contexts by taking a model-agnostic, game theoretical approach and considering the marginal contribution to a prediction of each individual model feature. In the case of the QVAR, model features are the included endogenous and exogenous variables.[15] Shapley values are often used in the machine learning literature for similar purposes, as described by Lundberg and Lee (2017), and have started to gain traction within macroeconomic time series analysis (e.g. Borup et al. (2022)). In standard machine learning applications, Shapley values are computed by re-training or re-estimating the model for each permutation of feature combinations. Instead of re-estimating the QVAR for each combination of model features we fix the model parameters to the full model estimates across permutations. By doing so, we avoid a potential interpretation issue, whereby the inclusion or exclusion of a model feature is attributed explanatory power not just through its movement over time, but also its impact on the parameter estimates of other model features. This, in turn, makes it easier to apply economic interpretation to the Shapley values in a manner closer, although not necessarily equivalent, to that of standard forecast error variance decomposition (e.g. Lütkepohl (1990)) used for linear VAR models, where the full model estimates are also taken as given.[16]

[14] A more detailed explanation of the Shapley value decomposition is given in appendix C.

[15] In principle, the QVAR could be further partitioned into individual lags for each endogenous and exogenous variable, yielding a total of $K \cdot P + M \cdot (S + 1)$ model features. For the sake of computational feasibility as well as interpretability, we do not distinguish between lags when computing Shapley values.

[16] Keeping the parameters fixed instead of re-estimating them to obtain Shapley values has no substantial implications for the qualitative results of the decomposition.

Figure 7: Shapley value decomposition of select conditional quantile forecasts for in the baseline and counterfactual scenario

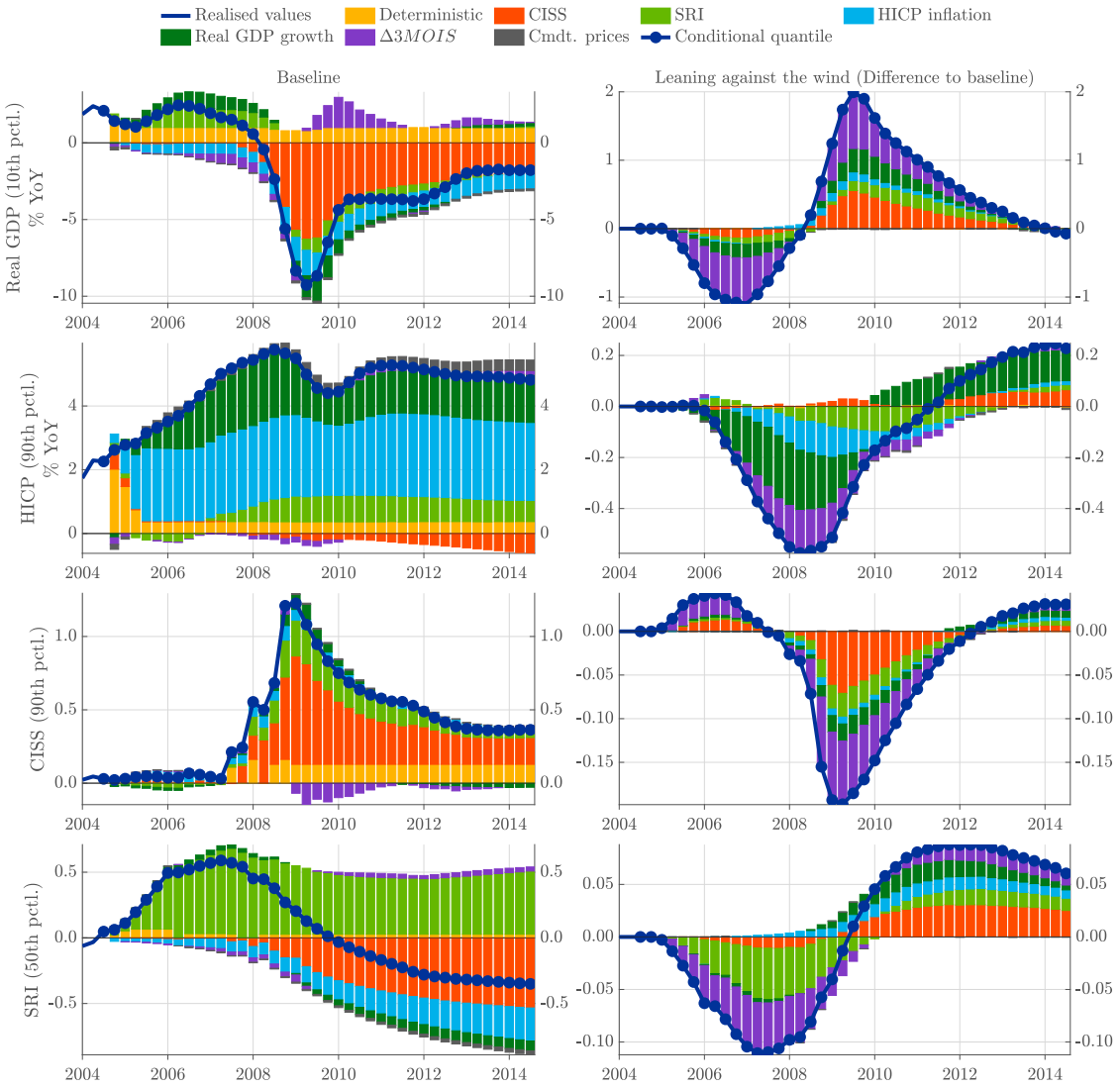

Source: ECB and authors' calculations.
Note: Shapley values are computed jointly for all lags of a given variable and do not distinguish between each lag for each variable. All $K \cdot 2^{K+M}$ model evaluations are based on 100.000 forward simulations and employ the estimated parameters from the full model specification. Slight differences between the sum of Shapley values and the conditional quantiles can occur due to Monte Carlo error. 'Deterministic' covers constant terms and, to the extent relevant, exogenous shocks and historical values from conversion of quarterly to annual growth rates.

Figure 7 plots the Shapley value decomposition of select conditional quantiles in the baseline as well as the change to the counterfactual policy scenario.[17] Starting with the left hand side,

[17]Shapley value decompositions of the 10th, 50th and 90th conditional quantile forecasts for all endogenously determined variables in the baseline scenario can be found in figure A.7 in appendix A.

downside risks to growth are, unsurprisingly, driven by the CISS and the SRI, both during the boom, where negligible levels of stress and increasing imbalances supports growth, as well as the bust, where deleveraging and systemic stress exacerbate the downturn. Financial factors play a limited role for upside risks to inflation where commodity prices, output growth and own dynamics exert particular influence. Additionally, monetary policy in the baseline is largely inconsequential, having limited and delayed impacts on growth- and inflation-at-risk.[18]

In the counterfactual policy scenario, downside risks to growth are initially increasing compared to the baseline as monetary policy tightens. However, as higher rates curb the build-up of systemic vulnerabilities, systemic stress is partially contained at the onset of the crisis. Ultimately, figure 7 shows that leaning against the wind in the QVAR would have resulted in a maximum reduction in downside risks to growth of close to 2 percentage points year-on-year, not only because of the accommodating effects of monetary policy working through the traditional channels, but also due to a reduction in systemic vulnerabilities in the pre-crisis period. Notably, leaning against the wind has an asymmetric effect on the conditional distribution of growth, with the lower quantiles benefiting more than the rest of the distribution (See figure A.8 in appendix A).

Using the QVAR, the analysis above makes it clear that monetary policy makers can potentially reduce the adverse impact of a severe financial crisis on growth by leaning against the wind early on. However, as stated previously, this necessarily requires policy makers to accept lower growth and inflation and potential deviations from related target levels in the upswing. To gauge this trade-off, consider a monetary policy maker facing the optimisation problem,

$$\begin{aligned} \underset{\Omega_t}{min}\ \frac{1}{2}\mathbb{E}_0\left[\sum_{t=0}^{\infty}\rho^t\left[\begin{array}{c} a\mathcal{I}\left(\pi_t<\pi^-\right)\left(\pi^- - \pi_t\right)^{\alpha} + (1-a)\,\mathcal{I}\left(\pi_t>\pi^+\right)\left(\pi_t-\pi^+\right)^{\beta} \\ +w_y\left(b\mathcal{I}\left(y_t<y^-\right)\left(y^- - y_t\right)^{\gamma} + (1-b)\,\mathcal{I}\left(y_t>y^+\right)\left(y_t-y^+\right)^{\delta}\right)\end{array}\right]\right] \\ s.t. \\ \pi_t = \pi\left(\Omega_t\right),\ y_t = y\left(\Omega_t\right) \end{aligned} \tag{4}$$

letting ρ be the usual discount factor. The loss function in (4) is that of Kilian and Manganelli (2008) and ensures congruence between the risk management model of central banking and the standard minimisation of loss problem in the literature. In particular, letting $\mathcal{I}(\cdot)$ denote the

[18] One should be cautious when interpreting Shapley values for more heavily restricted variables, in particular the CISS and SRI in the baseline, as shifting quantile restrictions can lead to notable jumps in Shapley values as the underlying model parameters are changing in line with the restrictions.

indicator function, a central banker acting as a risk manager of the macroeconomy minimises expected loss using its set of policy instruments, Ω, by keeping inflation, π_t, and output growth, y_t, within a predefined set of tolerance bands, $[\pi^-;\pi^+]$ and $[y^-;y^+]$, respectively. Outcomes outside of these bands are suboptimal, and the central banker may view positive and negative deviations differently. For instance, a central banker may be more averse to a 3 percentage point negative deviation of growth than a positive deviation of similar size, while inflation undershooting could be perceived as worse than the opposite case given the risk of hitting the effective lower bound of policy rates and entering into a deflationary trap. The balance of these risks are given by the weights, $0 \leq a, b \leq 1$ while w_y is the relative weight of output against inflation in the loss function.[19]

Figure 8 plots the effects on the central banker's expected loss of monetary policy leaning against the financial cycle at each forward horizon using the loss function in (4). To fix ideas, we set $\pi^- = \pi^+ = 2$ and $y^- = y^+ = 0$, denoting growth and inflation in year-on-year percentages, while $a = 0.5$ and $b = 1$, meaning the central banker cares equally about upside and downside deviations of inflation, but only cares about negative growth. Finally, we set $\rho = 0.98^{\frac{1}{4}}$, $w_y = 0.5$ and $\alpha = \beta = \gamma = \delta = 2$.

The left hand chart shows the impact of a broad based "leaning" where both preemptive tightening and crisis management is employed. In this setup, preemptive tightening initially increases the risk of inflation undershooting its lower tolerance, π^-, relative to the reduction in excessive inflation risk, as well as the risk of lower growth, thereby increasing the short-term expected loss. But the additional policy easing from crisis management to combat the jump in financial stress decreases the expected loss substantially by curbing downside risks to growth and reducing disinflationary pressures from the downturn, nearly cancelling out the additional losses from undershooting inflation during the build-up. The right-hand chart shows the change in expected loss in a counterfactual where policymakers hike rates preemptively to lower systemic risks but do not engage in additional monetary easing during the crisis compared to the baseline. Notably, simply limiting the build-up of systemic risks leads to a preferable outcome from the central banker's point of view.

It should be stressed, however, that the cost-benefit analysis above is conducted ex post, taking the onset of a financial crisis for granted. In a real-time, ex ante context, most relevant

[19] Since we are only considering the monetary policymakers' problem, we do not explicitly include tail risks in the loss function which would be more relevant for macroprudential policy, see e.g. Carney (2020).

Figure 8: Change in the central bank loss function by leaning against the wind

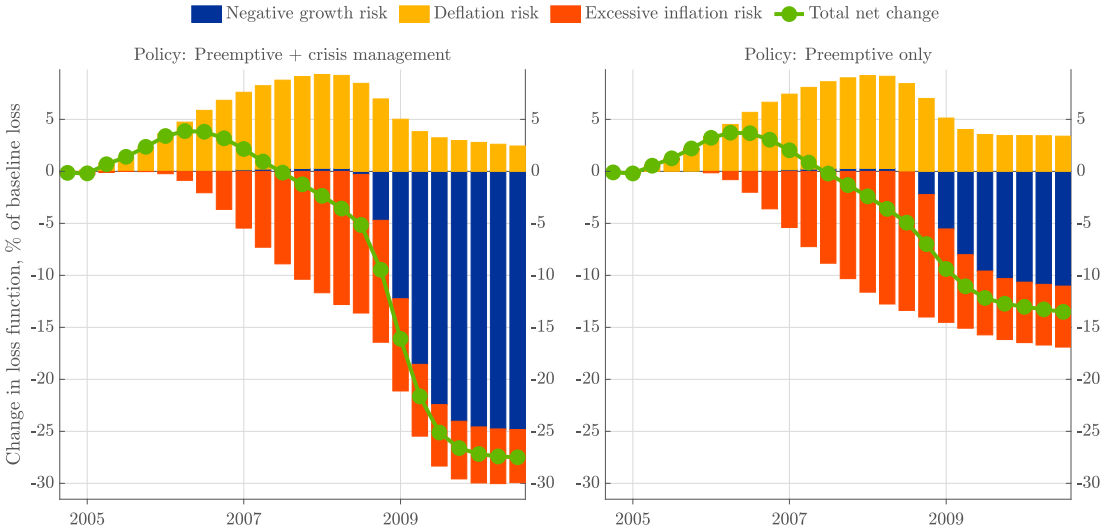

Source: Authors' calculations.
Note: Based on 10^6 forward simulations using 2004Q3 as forecast origin.

to policy makers, there is only a certain probability that a crisis will occur, and a counterfactual analysis would necessarily involve evaluating a leaning policy over a range of plausible probability-weighted scenarios, especially those in which a financial crisis both does and does not materialise as a possible consequence of increased financial imbalances. If the probability of a financial crisis is judged to be low, then leaning against the wind may prove too costly in expectation, even if it provides a net benefit in the event of a crisis. We leave this type of ex ante analysis outside of the scope of this paper, as it would require a careful calibration of the crisis and the non-crisis scenarios, including an assumed path of the crisis probability during the build-up phase, which could be made dependent on the SRI.

7 Monetary policy trade-offs when inflation emerges

We now turn to a scenario in which the central bank faces both rising inflation above its target value and an increase in financial stress. Specifically, we base our scenario on the macro-financial environment prevailing in the euro area in 2022, characterised by a rapid increase in monetary policy rates by the ECB against the background of initially supply-driven inflationary pressures accompanied by a slowdown in growth and elevated levels of financial stress, in part explained by the war in Ukraine starting in February 2022 as well as uncertainty about the persistence of

the inflationary bout. In this setting, the intratemporal financial stability and inflation-output trade-offs combine into an inflation-financial stability trade-off, greatly complicating the central banker's task, who must now decide whether to ease monetary policy to contain stress in the financial system at the risk of higher inflation, or further tighten monetary policy to rein in inflation at the cost of potentially triggering or amplifying systemic strains.

7.1 Calibration

Our conditional forecast uses 2022Q3 as forecast origin and runs a little more than four years, starting from 2022Q4 and ending in 2026Q4. To anchor the path for expected interest rates, we compute 3-month forward rates until 2024Q4 based on the EUR OIS term structure at the end of 2022Q3. Restricting the mean QVAR projection to equal the market implied rates as described in appendix B, figure 9 plots the projected conditional forward distribution against recent historical observations. At the end of 2022Q3 markets expected the ECB to hike rates more forcefully through 2023, after which short-term rates would settle at a terminal value of around 3.3 percent.

We assume commodity price inflation develops over the forecast horizon in line with the assumptions underlying the downside scenario of the ECB's publicly available macroeconomic projection exercise (MPE) in 2022Q3.[20] We could have used alternative commodity price assumptions but have chosen the present one for convenience. The resulting forward distribution for commodity price inflation is depicted in figure 9, and computed by transposing projections of individual commodity prices from the MPE into index projections using the publicly available index weights. Commodity prices are assumed to continue increasing for the next few years, though at a decelerating pace until a new equilibrium level is reached in 2025.

Lastly, while we do not impose any additional shocks to the CISS, we can think of the its initial climb and subsequent persistence as partly representing an inflation scare, where the central bank's commitment to containing inflation is put into question, causing an increase in government bond yields and volatility. As argued by Goodfriend (1993) and Goodfriend (1998), inflation scares contributed non-negligibly to several episodes of heightened volatility in US Treasury markets during the 1970's and 1980's.

As the central bank's choice between expansionary or contractionary monetary policy is less obvious in the macroeconomic environment underlying this scenario, we conduct a sensitivity

[20] See European Central Bank (2016) for a description of the projection exercise.

Figure 9: Projections for the 3-month EUR OIS rate and commodity prices

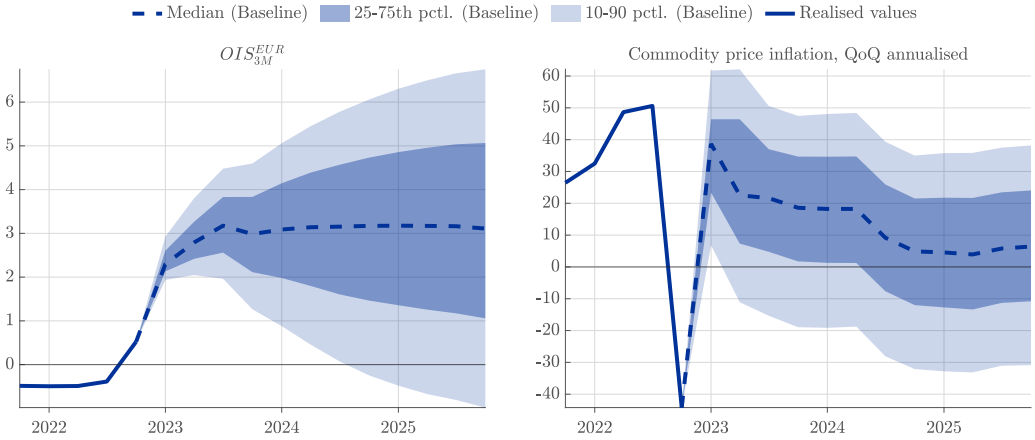

Source: ECB, Haver Analytics, Refinitiv and authors' calculations.
Note: The left hand chart plots the QVAR-generated conditional forward distribution centered around inferred 3-month forward rates based on EUR OIS market prices. The right hand chart shows the QVAR-generated forward distribution of seasonally adjusted commodity price inflation centered around MPE projections. Based on 10^6 forward simulations using 2022Q3 as forecast origin.

analysis that revolves around assumptions of both loser and tighter monetary policy. Specifically, we consider four consecutive quarters of 25 basis points additional rate increases and decreases, respectively compared to the baseline path, beginning in 2022Q4. As a result, the expected short-term interest rates level off at 'terminal' values exactly 1 percentage point higher and lower, respectively, than the terminal rate of the baseline assumption.

7.2 Results

Figure 10 charts as solid lines the conditional forecasts for the four endogenously determined variables in the baseline scenario for the 10th, the 50th and the 90th quantiles of the conditional forecast distributions. The dotted and the dashed series around those baseline quantiles reflect the outcomes of the sensitivity analysis. Figure 11 provides information on the driving factors behind the baseline projections for real GDP growth and HICP inflation for the same quantiles, again using Shapley value decompositions.[21] A few points are worth highlighting.

Downside risks to growth are notably affected in this scenario, reaching -9% in 2024 in the baseline (Figure 10). Downside risks to growth are particularly driven by the elevated CISS and inflation levels as well as the embedded monetary tightening.

[21] Shapley value decompositions of the 10th, 50th and 90th conditional quantile forecasts for all endogenously determined variables in the baseline scenario can be found in figure A.9 in appendix A.

Figure 10: Conditional quantile forecasts of real and financial variables with and without additional monetary policy measures

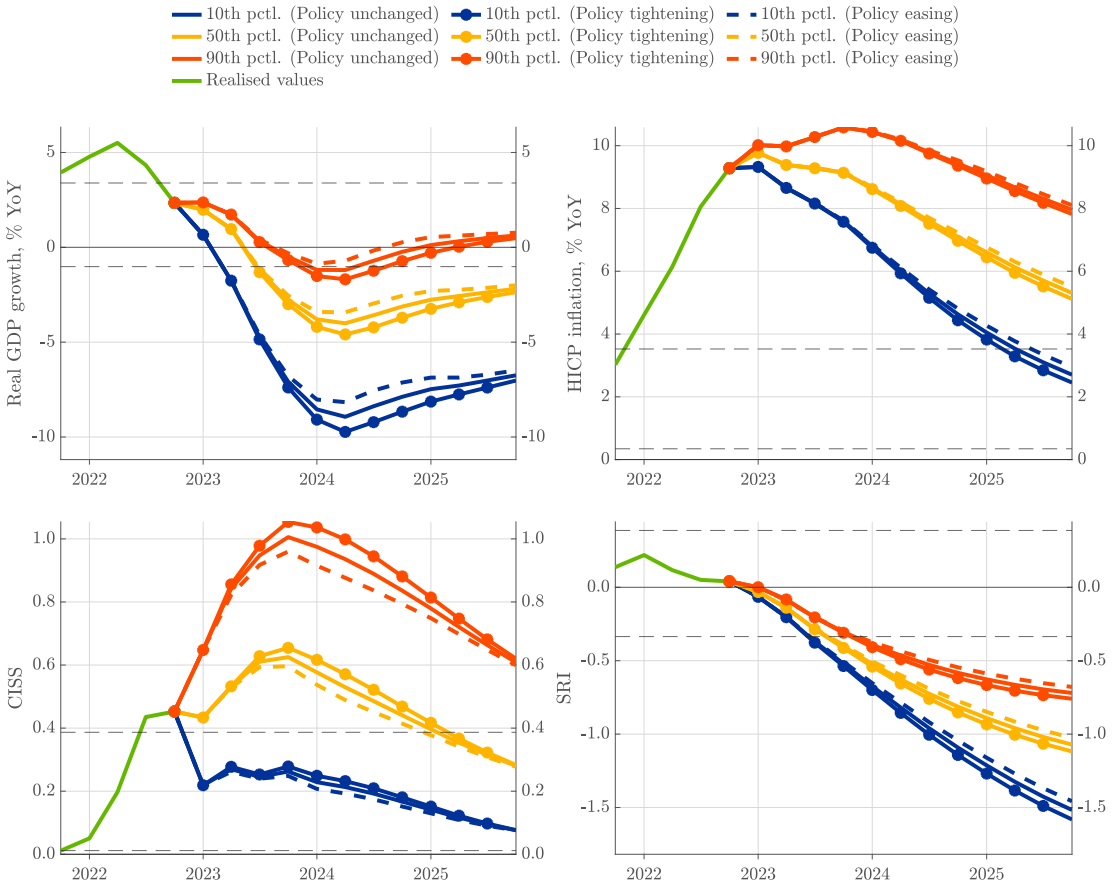

Source: ECB and authors' calculations.
Note: Based on 10^6 forward simulations using 2022Q3 as forecast origin. While the CISS is constructed to take values in the intervals $[0; 1]$, it is not immediately possible to impose this restriction in the QVAR framework, causing some quantiles forecasts to lie outside their respective boundaries. Horizontal dashed lines indicate the 10th and 90th unconditional percentiles, respectively.

The projected quantiles of inflation are largely explained by past inflation developments via own lags, which we interpret as supply-side factors such as price stickiness and updating of inflation expectations, for instance. As expected, the assumption of further increases in commodity prices puts additional upwards pressure on inflation across its entire conditional distribution. For instance, inflation-at-risk (the 90th quantile) peaks in the first half of 2023 just above 10% year-on-year and only slowly falls to around 6% in 2026. Median inflation is projected to decline more quickly from close to 10% at the outset to about 4% in 2026 (Figure 11).

As expected, the monetary policy tightening (easing) in excess of what is priced in by the

market at the forecast origin tends to lower (increase) the conditional forecast distributions of both growth and inflation, with lower growth quantiles affected relatively more. In particular, growth-at-risk is reduced (increased) by approximately 1%, while inflation-at-risk is reduced (increased) by around 0.2%.

Figure 11: Shapley value decomposition of select conditional quantile forecasts for real GDP growth and HICP inflation in the baseline

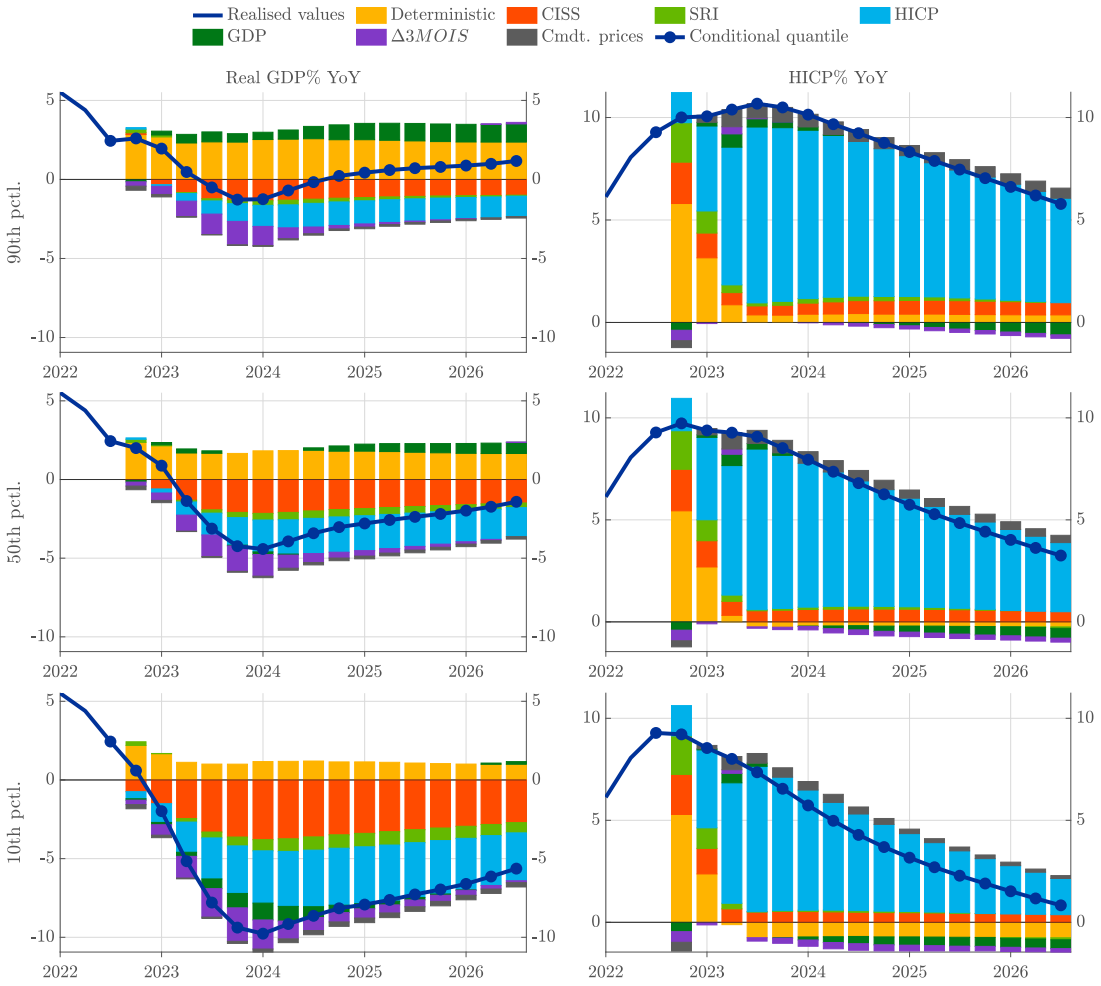

Source: ECB and authors' calculations.
Note: Shapley values are computed for all lags pertaining to a given variable and do not distinguish between each lag for each variable. All $K \cdot 2^{K+M}$ model evaluations are based on 100.000 forward simulations and employ the estimated parameters from the full model specification. Slight differences between the sum of Shapley values and the conditional quantiles can occur due to Monte Carlo error. 'Deterministic' covers constant terms and, to the extent relevant, exogenous shocks and historical values from conversion of quarterly to annual growth rates.

In the financial stability block, the CISS is primarily driven by own dynamics, while the SRI trends downward, possibly reflecting increased financial stress as well as elevated inflation

Figure 12: Change in the central bank loss function by tightening and easing monetary policy

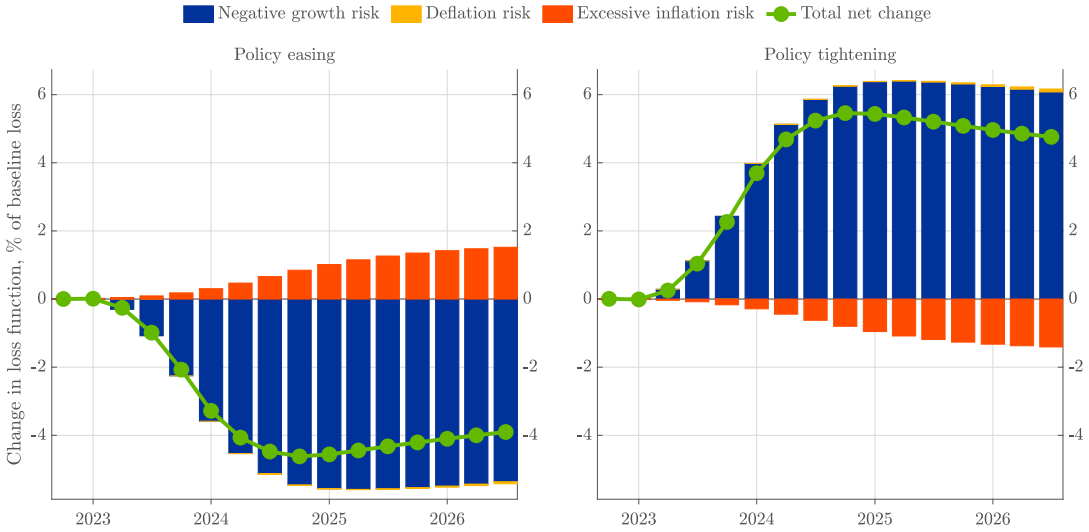

Source: Authors' calculations.
Note: Based on 10^6 forward simulations using 2022Q3 as forecast origin.

attenuating financial imbalances through a drop in real asset prices and credit provision. Tighter (easier) monetary policy tends to exacerbate (decrease) upside risks to the CISS and induce further (less) systemic deleveraging. In any case, the projected worsening of financial stability conditions and the associated elevated downside risks for economic activity seem to represent a very unfavourable price stability-financial stability trade-off under both policy alternatives.

Like the last section, figure 12 illustrates the implications for the central bank loss function of the two different monetary policy paths using the previously established framework. Easier monetary policy (left-hand chart) generates lower expected losses driven by the associated decrease in downside risks to growth despite its positive impact on inflation. Conversely, additional monetary tightening (right-hand chart) contributes to higher losses in the medium term, as the relatively muted impact on inflation is more than offset by the increased downside risks to growth generated by the rate hikes and the fact there there is practically zero risk of undershooting the inflation target.

In the face of dramatic cost-push shocks and increased financial stress as experienced in the latter half of 2022, the analysis above thus suggests that the central bank would prefer sacrificing price stability for output stabilisation as the costs of reducing inflation measured in growth-at-risk, essentially a quantile version of the 'sacrifice-ratio', are simply too great to bear when

deteriorating financial stability conditions weigh particularly strongly on the downside risks to growth. On the other hand, the extra losses from a tighter monetary policy would become lower, or may even turn into net benefits, for a central bank that puts relatively more weight on achieving its inflation target rather than avoiding negative growth, in our framework a low value of w_y. For instance, the ECB specifically has no direct growth mandate but one that explicitly commands the ECB to focus on price stability. Transposing the ECB's lexicographic preference ordering into the extreme case of a zero weight on output deviations in its loss function would then favour tighter monetary policy in response to the recent inflationary pressures despite the adverse implications for financial stability and growth-at-risk.

Another factor that is not considered in the analysis is the limited sample of euro area data on which the QVAR is estimated and from which it follows that inflation is a globally stationary process, even if individual quantiles may exhibit unit root behaviour. Quantile reversion, in turn, implies that the conditional forecast distribution of inflation will always return to more "tolerable" levels eventually, and under this pretext it may make sense for the central bank to mitigate short-term adverse outcomes on growth as losses from inflation will abate with time. However, stationarity of inflation as observed in the data can arguably be attributed, at least in part, to the successful anchoring of inflation expectations by policy makers over the sample period. As such, persistently high inflation may induce a de-anchoring of inflation expectations, which cannot be captured by the QVAR because it is not in the historical data. Monetary policy internalising this potential outcome may therefore be inclined to favour a tighter policy stance, even if they attach a non-zero weight to stabilising output growth, because the potential costs of deanchored inflation expectations may potentially outweigh the short term losses from tightening (e.g. Schnabel (2022)).

8 Conclusion

In this paper, we present an empirical framework for informing monetary policy about the short- to medium-term macroeconomic implications of different financial stability conditions and the extent to which monetary policy can influence such macroeconomic outcomes in pursuit of its policy mandate. The nonlinearity of the framework applied makes it particularly suitable for a risk management approach to monetary policy, which focuses on balancing the potentially asymmetric upside and downside risks to its main variables of interest. There are more practical

policy applications of the model than those presented in the paper. For example, the QVAR could also be used to generate non-trivial conditional forecast distributions around the conventional median or mean macroeconomic projections produced by central banks and other policy authorities or research institutes. This could add reliability to an assessment of the projection risks based on a satellite model that still produces consistent central projections. Of course, our empirical model is rather stylised and can therefore only be seen as a first step in the intended direction of policy use. Given the curse of dimensionality in quantile regressions and the typically small data samples available, the model estimation may benefit from the application of Bayesian techniques to obtain more precise coefficient estimates for potentially more parameters when aiming at a more sophisticated modelling of the financial, real or monetary policy blocks of the QVAR.

References

[1] Acharya, V. V., Chauhan, R. S., Rajan, R. G., and Steffen, S. (2023). Liquidity dependence and the waxing and waning of central bank balance sheets. *NBER Working Paper*, 31050.

[2] Acharya, V. V., Engle, R. F., and Steffen, S. (2021). Why did bank stocks crash during covid-19? *NBER Working Paper*, 28559.

[3] Adrian, T., Boyarchenko, N., and Giannone, D. (2019). Vulnerable growth. *American Economic Review*, 109(4):1263–89.

[4] Adrian, T., Grinberg, F., Liang, N., Malik, S., and Yu, J. (2022). The term structure of growth-at-risk. *American Economic Journal: Macroeconomics*, 14(3):283–323.

[5] Adrian, T. and Liang, N. (2016). Monetary policy, financial conditions, and financial stability. *International Journal of Central Banking*, 14(1).

[6] Alessi, L. and Detken, C. (2018). Identifying excessive credit growth and leverage. *Journal of Financial Stability*, 35:215–225.

[7] Antolin-Diaz, J., Petrella, I., and Rubio-Ramirez, J. F. (2021). Structural scenario analysis with SVARs. *Journal of Monetary Economics*, 117:798–815.

[8] Bagehot, W. (1873). *Lombard street*. King.

[9] Bassett Jr, G. and Koenker, R. (1982). An empirical quantile function for linear models with iid errors. *Journal of the American Statistical Association*, 77(378):407–415.

[10] Bauer, M. D., Bernanke, B. S., and Milstein, E. (2023). Risk appetite and the risk-taking channel of monetary policy. *Journal of Economic Perspectives*, 37(1):77–100.

[11] Bernanke, B. S. (2015). Federal Reserve policy in an international context. Paper presented at the 16th Jacques Polak Annual Research Conference hosted by the International Monetary Fund, Washington, D.C., November 5–6, 2015.

[12] Boissay, F., Collard, F., Galí, J., and Manea, C. (2021). Monetary policy and endogenous financial crises. *NBER Working Paper*, 29602.

[13] Borio, C. (2010). Ten propositions about liquidity crises. *CESifo Economic Studies*, 56(1):70–95.

[14] Borup, D., Coulombe, P. G., Rapach, D., Schütte, E. C. M., and Schwenk-Nebbe, S. (2022). The anatomy of out-of-sample forecasting accuracy. *Federal Reserve Bank of Atlanta Working Paper*, 2022-16.

[15] Boyarchenko, N., Favara, G., and Schularick, M. (2022). Financial stability considerations for monetary policy: empirical evidence and challenges. *FEDS Working Paper*, 2022-006.

[16] Brandao-Marques, L., Gelos, G., Narita, M., and Nier, E. (2020). Leaning against the wind: A cost-benefit analysis for an integrated policy framework. *IMF Working Paper*, WP/20/123.

[17] Carney, M. (2020). The grand unifying theory (and practice) of macroprudential policy. Speech given by Mark Carney, Governor of the Bank of England, Logan Hall, University College London, 5 March 2020.

[18] Cavallino, P., Cornelli, G., Hördahl, P., and Zakrajsek, E. (2022). "Front-loading" monetary tightening: pros and cons. *BIS Bulletin*, 63.

[19] Chavleishvili, S., Engle, R. F., Fahr, S., Kremer, M., Manganelli, S., and Schwaab, B. (2021). The risk management approach to macro-prudential policy. *ECB Working Paper*, 2565.

[20] Chavleishvili, S. and Kremer, M. (2023). Measuring systemic financial stress and its risks for growth. *ECB Working Paper*, forthcoming.

[21] Chavleishvili, S. and Manganelli, S. (2019). Forecasting and stress testing with quantile vector autoregression. *ECB Working Paper*, 2330.

[22] Chavleishvili, S. and Mönch, E. (2023). Natural disasters as macroeconomic tail risks. Mimeo.

[23] Chernozhukov, V., Fernández-Val, I., and Galichon, A. (2010). Quantile and probability curves without crossing. *Econometrica*, 78(3):1093–1125.

[24] Christiano, L. J., Eichenbaum, M., and Evans, C. L. (1999). Monetary policy shocks: what have we learned and to what end? *Handbook of Macroeconomics*, 1:65–148.

[25] Clarida, R. H. and Coyle, D. (1984). Conditional projection by means of Kalman filtering. *NBER Technical Working Paper*, 36.

[26] Coibion, O. and Gorodnichenko, Y. (2012). Why are target interest rate changes so persistent? *American Economic Journal: Macroeconomics*, 4:126–162.

[27] de Bandt, O. and Hartmann, P. (2001). Systemic risk: a survey. In Goodhart, C. and Illing, G., editors, *Financial crisis, contagion and the lender of last resort: A book of readings*, pages 249–298. Oxford University Press.

[28] Doan, T., Litterman, R., and Sims, C. (1984). Forecasting and conditional projection using realistic prior distributions. *Econometric Reviews*, 3(1):1–100.

[29] Estrella, A. (2015). The price puzzle and VAR identification. *Macroeconomic Dynamics*, 19(8):1880–1887.

[30] European Central Bank (2016). A guide to the Eurosystem/ECB macroeconomic projection exercises. Technical report, European Central Bank.

[31] European Central Bank (2021). The role of financial stability considerations in monetary policy and the interaction with macroprudential policy in the euro area. *European Central Bank, Occasional Paper Series*, 272.

[32] Fagan, G., Henry, J., and Mestre, R. (2005). An area-wide model for the euro area. *Economic Modelling*, 22(1):39–59.

[33] Filardo, A. and Rungcharoenkitkul, P. (2016). A quantitative case for leaning against the wind. *BIS Working Paper*, 594.

[34] Fitzenberger, B. (1998). The moving blocks bootstrap and robust inference for linear least squares and quantile regressions. *Journal of Econometrics*, 82(2):235–287.

[35] Freixas, X., Laeven, L., and Peydró, J.-L. (2015). *Systemic risk, crises, and macroprudential regulation*. The MIT Press.

[36] Giannone, D., Lenza, M., and Reichlin, L. (2019). Money, credit, monetary policy and the business cycle in the euro area: what has changed since the crisis? *International Journal of Central Banking*, 15(5):137–173.

[37] Goldberg, J. E., Klee, E., Prescott, E. S., and Wood, P. R. (2020). Monetary policy strategies and tools: financial stability considerations. *FEDS Working Paper*, 2020-074.

[38] Goodfriend, M. (1993). Interest rate policy and the inflation scare problem: 1979-1992. *Federal Reserve Bank of Richmond Economic Quarterly*, 79(1):1–23.

[39] Goodfriend, M. (1998). Using the term structure of interest rates for monetary policy. *Federal Reserve Bank of Richmond Economic Quarterly*, 84(3):13–30.

[40] Gourio, F., Kashyap, A. K., and Sim, J. W. (2018). The trade offs in leaning against the wind. *IMF Economic Review*, 66:70–115.

[41] Grimm, M., Jordà, Ò., Schularick, M., and Taylor, A. M. (2023). Loose monetary policy and financial instability. *NBER Working Paper*, 30958.

[42] Hamilton, J. D. (2009). Understanding crude oil prices. *The Energy Journal*, 30(2):179–206.

[43] Hamilton, J. D. (2018). Why you should never use the Hodrick-Prescott filter. *The Review of Economics and Statistics*, 100(5):831–843.

[44] Härdle, W., Horowitz, J., and Kreiss, J.-P. (2003). Bootstrap methods for time series. *International Statistical Review*, 71(2):435–459.

[45] Hauser, A. (2022). Thirteen days in october: How central bank balance sheets can support monetary and financial stability. Speech given by Andrew Hauser, Executive Director for Markets of the Bank of England, European Central Bank, Frankfurt, 4 November 2022.

[46] Havranek, T. and Rusnak, M. (2013). Transmission lags of monetary policy: a meta-analysis. *International Journal of Central Banking*, 9(4):39–75.

[47] Hollo, D., Kremer, M., and Lo Duca, M. (2012). CISS - A composite indicator of systemic stress in the financial system. *ECB Working paper*, 1426.

[48] Inoue, A., Kilian, L., and Kiraz, F. B. (2009). Do actions speak louder than words? Household expectations of inflation based on micro consumption data. *Journal of Money, Credit and Banking*, 41(7):1331–1363.

[49] Jiang, E., Matvos, G., Piskorski, T., and Seru, A. (2023). Monetary tightening and U.S. bank fragility in 2023: mark-to-market losses and uninsured depositor runs? *NBER Working Paper*, 31048.

[50] Jordà, O., Schularick, M., and Taylor, A. M. (2013). When credit bites back. *Journal of Money, Credit and Banking*, 45:3–28.

[51] Jordà, O., Schularick, M., and Taylor, A. M. (2015). Leveraged bubbles. *Journal of Monetary Economics*, 76:S1–S20.

[52] Kashyap, A. K. and Stein, J. C. (2023). Monetary policy when the central bank shapes financial-market sentiment. *Journal of Economic Perspectives*, 37(1):53–76.

[53] Kilian, L. (2009). Not all oil price shocks are alike: disentangling demand and supply shocks in the crude oil market. *American Economic Review*, 99(3):1053–1069.

[54] Kilian, L. and Manganelli, S. (2008). The central banker as a risk manager: estimating the Federal Reserve's preferences under Greenspan. *Journal of Money, Credit and Banking*, 40(6):1103–1129.

[55] Kilian, L. and Vega, C. (2011). Do energy prices respond to us macroeconomic news? a test of the hypothesis of predetermined energy prices. *Review of Economics and Statistics*, 93(2):660–671.

[56] Kilian, L. and Vigfusson, R. J. (2013). Do oil prices help forecast US real GDP? the role of nonlinearities and asymmetries. *Journal of Business & Economic Statistics*, 31(1):78–93.

[57] Koenker, R. (2005). *Quantile regression*. Cambridge University Press.

[58] Koenker, R. and Bassett Jr, G. (1978). Regression quantiles. *Econometrica*, pages 33–50.

[59] Koenker, R., Chernozhukov, V., He, X., and Peng, L. (2017). *Handbook of quantile regression*. CRC press.

[60] Koenker, R. and Xiao, Z. (2006). Quantile autoregression. *Journal of the American Statistical Association*, 101(475):980–990.

[61] Koop, G., Pesaran, M. H., and Potter, S. M. (1996). Impulse response analysis in nonlinear multivariate models. *Journal of Econometrics*, 74(1):119–147.

[62] Lang, J. H., Izzo, C., Fahr, S., and Ruzicka, J. (2019). Anticipating the bust: a new cyclical systemic risk indicator to assess the likelihood and severity of financial crises. *ECB Working Paper*, 219.

[63] Lee, E. R., Noh, H., and Park, B. U. (2014). Model selection via Bayesian information criterion for quantile regression models. *Journal of the American Statistical Association*, 109(505):216–229.

[64] Leeper, E. M. and Zha, T. (2003). Modest policy interventions. *Journal of Monetary Economics*, 50(8):1673–1700.

[65] Lenza, M. and Primiceri, G. E. (2022). How to estimate a vector autoregression after March 2020. *Journal of Applied Econometrics*, 37(4):688–699.

[66] Lundberg, S. M. and Lee, S.-I. (2017). A unified approach to interpreting model predictions. In Guyon, I., Luxburg, U. V., Bengio, S., Wallach, H., Fergus, R., Vishwanathan, S., and Garnett, R., editors, *Advances in Neural Information Processing Systems*, volume 30. Curran Associates, Inc.

[67] Lütkepohl, H. (1990). Asymptotic distributions of impulse response functions and forecast error variance decompositions of vector autoregressive models. *The Review of Economics and Statistics*, 72(1):116–125.

[68] Machado, J. A. (1993). Robust model selection and M-estimation. *Econometric Theory*, 9(3):478–493.

[69] Martin, A. (2009). Reconciling bagehot and the fed's response to september 11. *Journal of Money, Credit and Banking*, 41(2-3):397–415.

[70] Mojon, B. and Peersman, G. (2001). A VAR description of the effects of monetary policy in the individual countries of the euro area. *ECB Working Paper*, 92.

[71] Richter, B., Schularick, M., and Wachtel, P. (2021). When to lean against the wind. *Journal of Money, Credit and Banking*, 53(1):5–39.

[72] Rusnák, M., Havranek, T., and Horváth, R. (2013). How to solve the price puzzle? a meta-analysis. *Journal of Money, Credit and Banking*, 45(1):37–70.

[73] Schnabel, I. (2022). Monetary policy and the great volatility. Speech by Isabel Schnabel, Member of the Executive Board of the ECB, at the Jackson Hole Economic Policy Symposium organised by the Federal Reserve Bank of Kansas City, Jackson Hole, Wyoming, 27 August 2022.

[74] Schularick, M. and Taylor, A. M. (2012). Credit booms gone bust: monetary policy, leverage cycles, and financial crises, 1870-2008. *American Economic Review*, 102(2):1029–1061.

[75] Schularick, M., ter Steege, L., and Ward, F. (2021). Leaning against the wind and crisis risk. *American Economic Review: Insights*, 3(2):199–214.

[76] Schüler, Y. S. (2020). The impact of uncertainty and certainty shocks. *Deutsche Bundesbank Discussion Paper*, 14/2020.

[77] Sims, C. A. (1992). Interpreting the macroeconomic time series facts: the effects of monetary policy. *European Economic Review*, 36(5):975–1000.

[78] Sims, C. A. and Zha, T. (2006). Does monetary policy generate recessions? *Macroeconomic Dynamics*, 10(2):231–272.

[79] Smets, F. (2018). Financial stability and monetary policy: how closely interlinked? *International Journal of Central Banking*, 10(2):263–300.

[80] Stein, J. (2013). Overheating in credit markets: origins, measurement, and policy responses. Speech given by Jeremy C. Stein, Governor of the Federal Reserve Board, "Restoring Household Financial Stability after the Great Recession: Why Household Balance Sheets Matter" research symposium, St. Louis, Missouri, 7 February 2013.

[81] Stein, J. C. and Sunderam, A. (2018). The fed, the bond market, and gradualism in monetary policy. *Journal of Finance*, 73(3):1015–1060.

[82] Svensson, L. E. (2017). Cost-benefit analysis of leaning against the wind. *Journal of Monetary Economics*, 90:193–213.

[83] Waggoner, D. F. and Zha, T. (1999). Conditional forecasts in dynamic multivariate models. *The Review of Economics and Statistics*, 81(4):639–651.

[84] Woodford, M. (2012). Inflation targeting and financial stability. *NBER Working Paper*, 17967.

A Additional figures

Figure A.1: Time series of quarterly euro area real GDP growth, 1990Q2:2022Q4

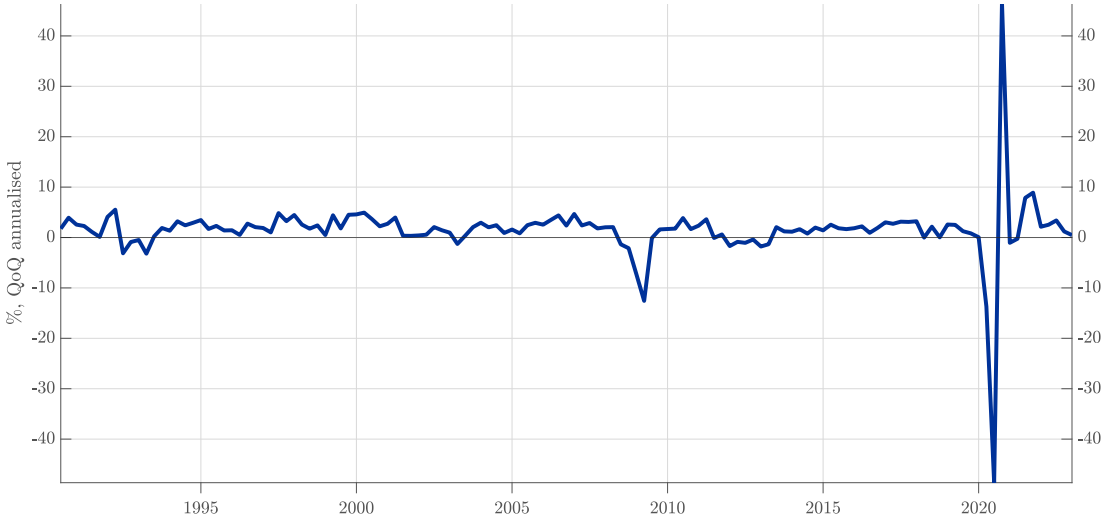

Source: ECB and authors' calculations.

Figure A.2: Time series of quarterly euro area HICP inflation, 1990Q2:2022Q4

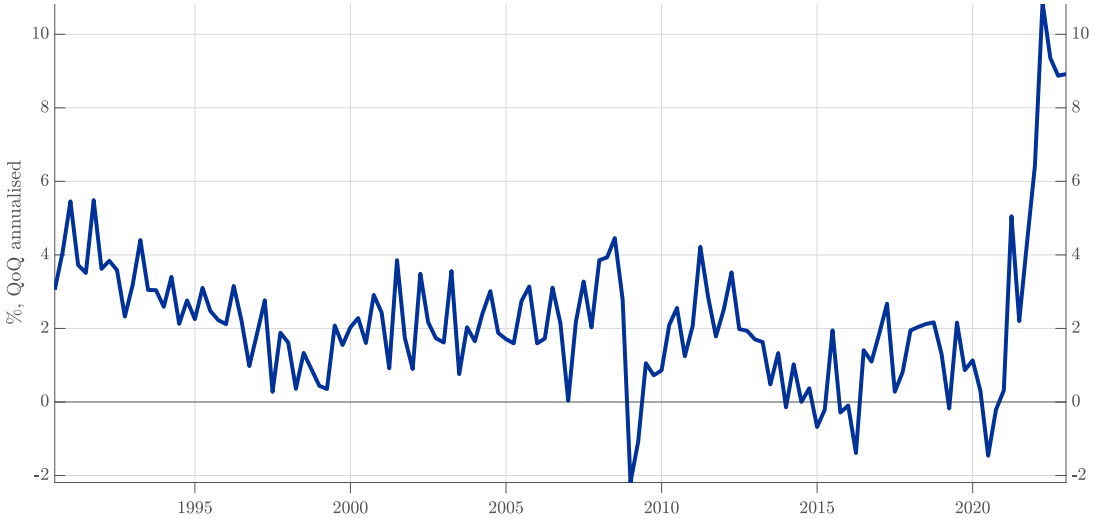

Source: ECB and authors' calculations.
Note: The series is constructed as 400 times the log difference between quarterly averages of the seasonally adjusted Harmonised Consumer Price Index for the euro area.

Figure A.3: Time series of the quarterly change in $OIS^{€}_{3M}$ rates, 1990Q2:2022Q4

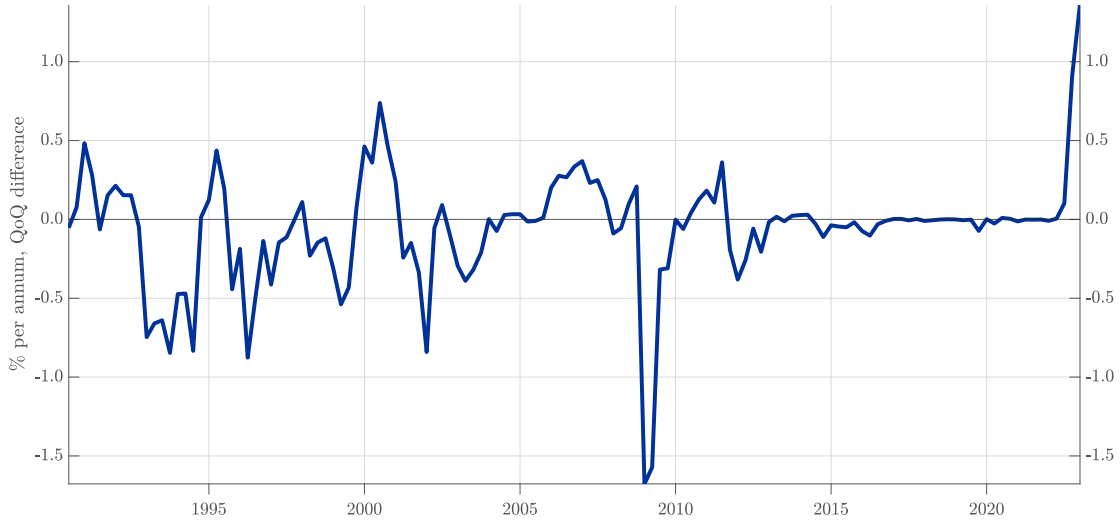

Source: ECB and authors' calculations.
Note: The series is constructed as the difference in quarterly averages of the the EUR 3M OIS rate. Before 2001, OIS rates are extrapolated from EURIBOR/FIBOR rates corrected for the average EURIBOR-OIS spread until 2007Q2.

Figure A.4: Time series of quarterly commodity price inflation, 1990Q2:2022Q4

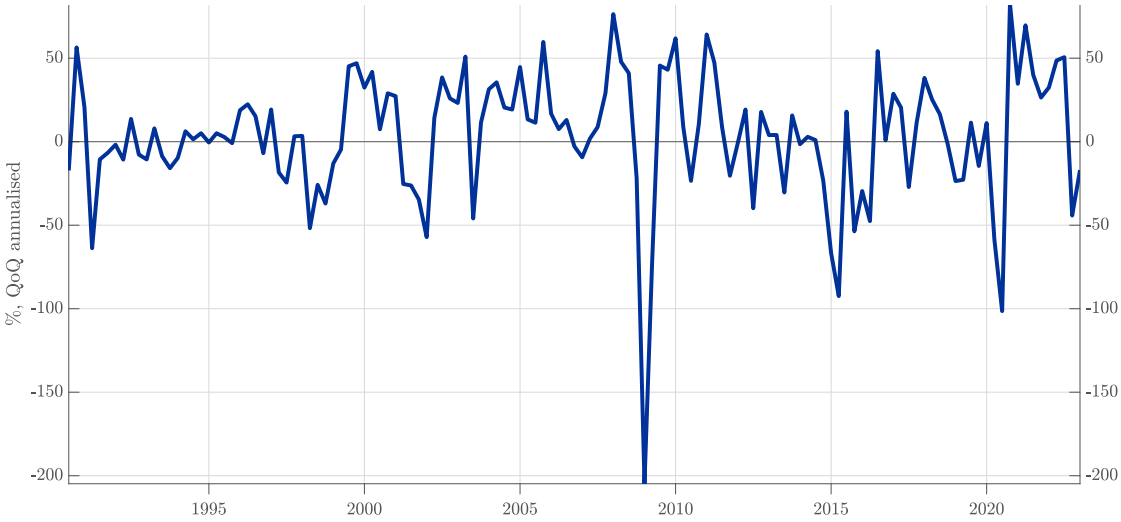

Source: ECB, Haver Analytics and authors' calculations.
Note: The series is constructed as 400 times the log difference between quarterly averages of the seasonally adjusted S&P GSCI index.

Figure A.5: G-QIRFs for shocks to endogenous variables

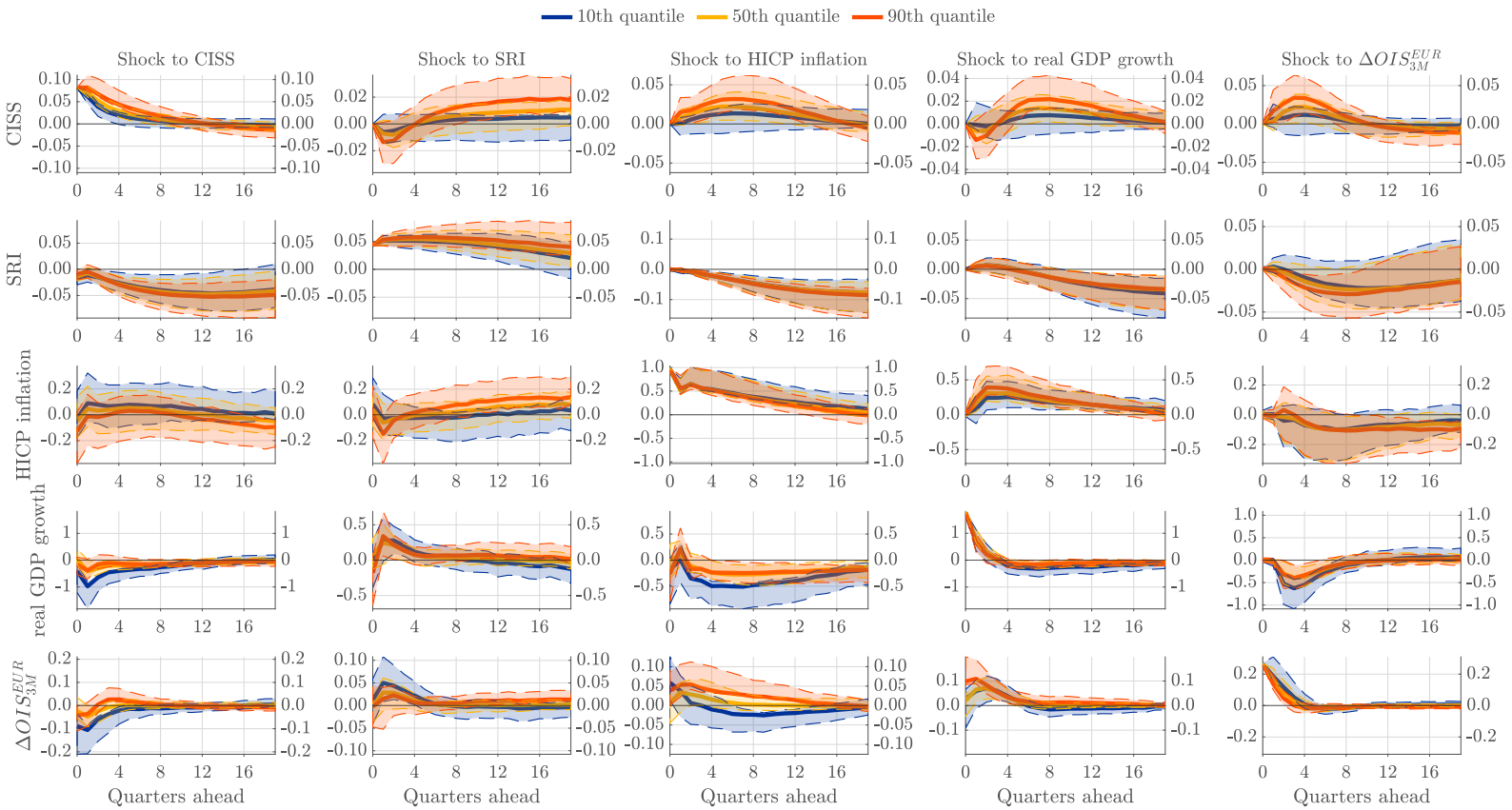

Source: ECB and authors' calculations.
Note: G-QIRFs for one standard deviation shocks based on 10^6. The shocks are set equal to the standard deviation of the errors in the QVAR equation for the respective variables at the 50th percentile. Initial conditions are set equal to the historical median values of the respective time series. Shaded areas indicate bootstrapped 90% confidence intervals using 5,000 bootstrap iterations with 2×10^4 forward simulations each.

Figure A.6: G-QIRFs for shocks to exogenous variables

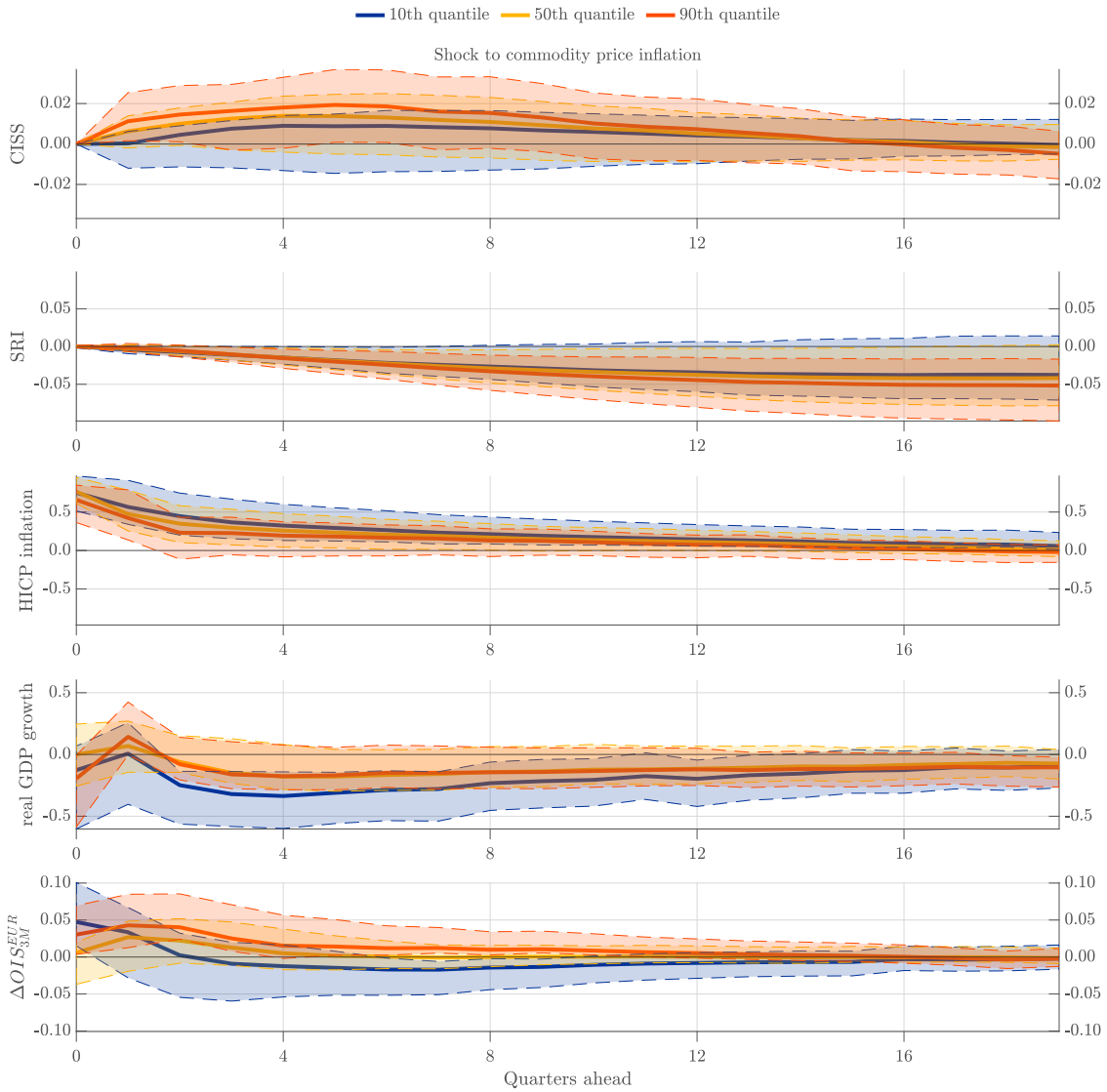

Source: ECB and authors' calculations.
Note: G-QIRFs for one standard deviation shocks based on 10^6 forward simulations. The shocks are set equal to the standard deviation of the errors in the QVAR equation for the respective variables at the 50th percentile. Initial conditions are set equal to the historical median values of the respective time series. Shaded areas indicate bootstrapped 90% confidence intervals using $5,000$ bootstrap iterations with 2×10^4 forward simulations each.

Figure A.7: Shapley value decomposition of select quantiles for endogenous variables in the financial crisis baseline scenario

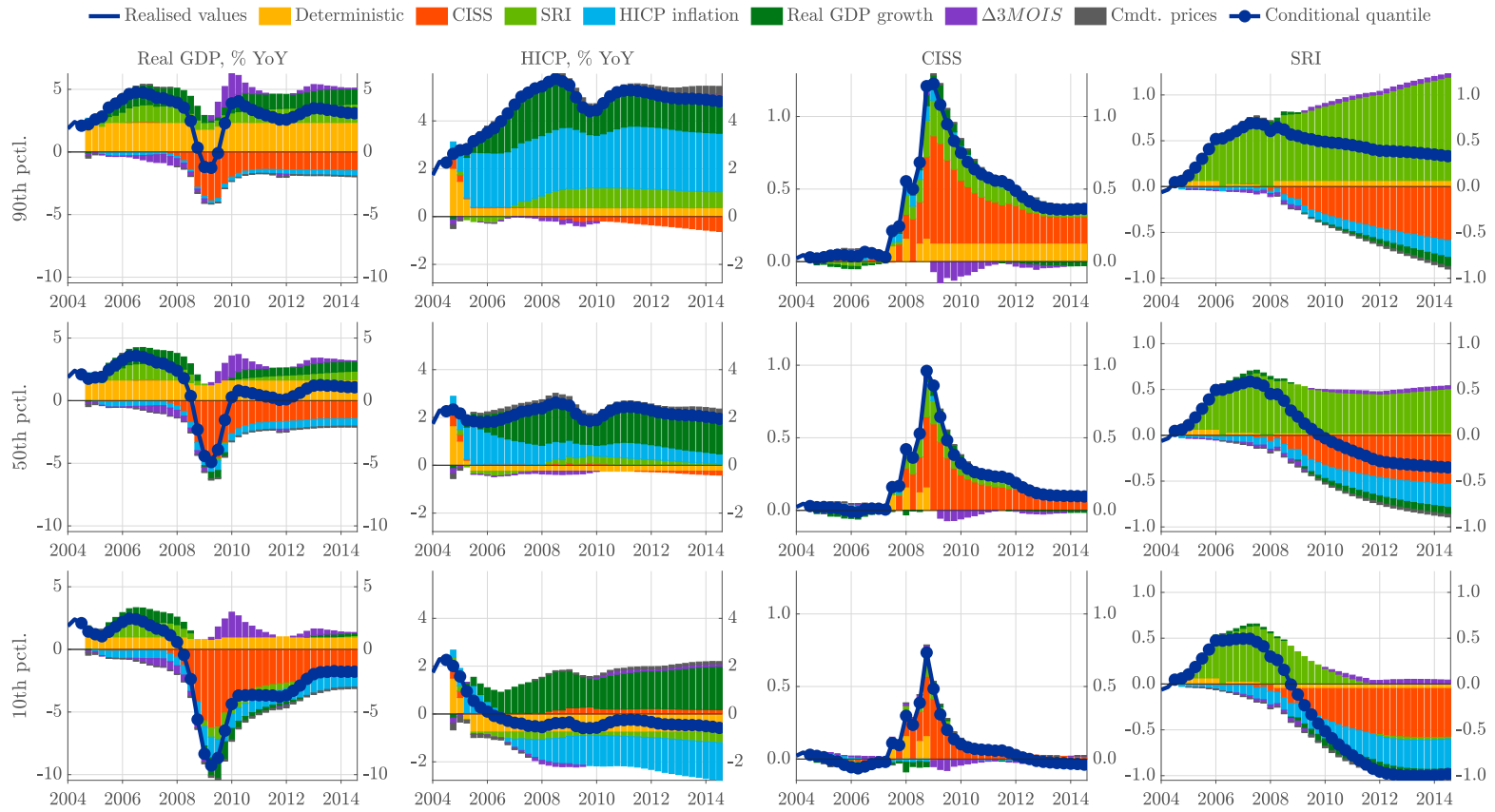

Source: ECB and authors' calculations.
Note: Shapley values are computed for all lags pertaining to a given variable and do not distinguish between each lag for each variable. All $K \cdot 2^{K+M}$ model evaluations are based on 100.000 forward simulations and employ the estimated parameters from the full model specification. Slight differences between the sum of Shapley values and the conditional quantiles can occur due to Monte Carlo error. 'Deterministic' covers constant terms and, to the extent relevant, exogenous shocks and historical values from conversion of quarterly to annual growth rates.

Figure A.8: Shapley value decomposition of the difference between select quantiles for endogenous variables in the financial crisis baseline scenario and the counterfactual with both preemptive tightening and crisis management policy

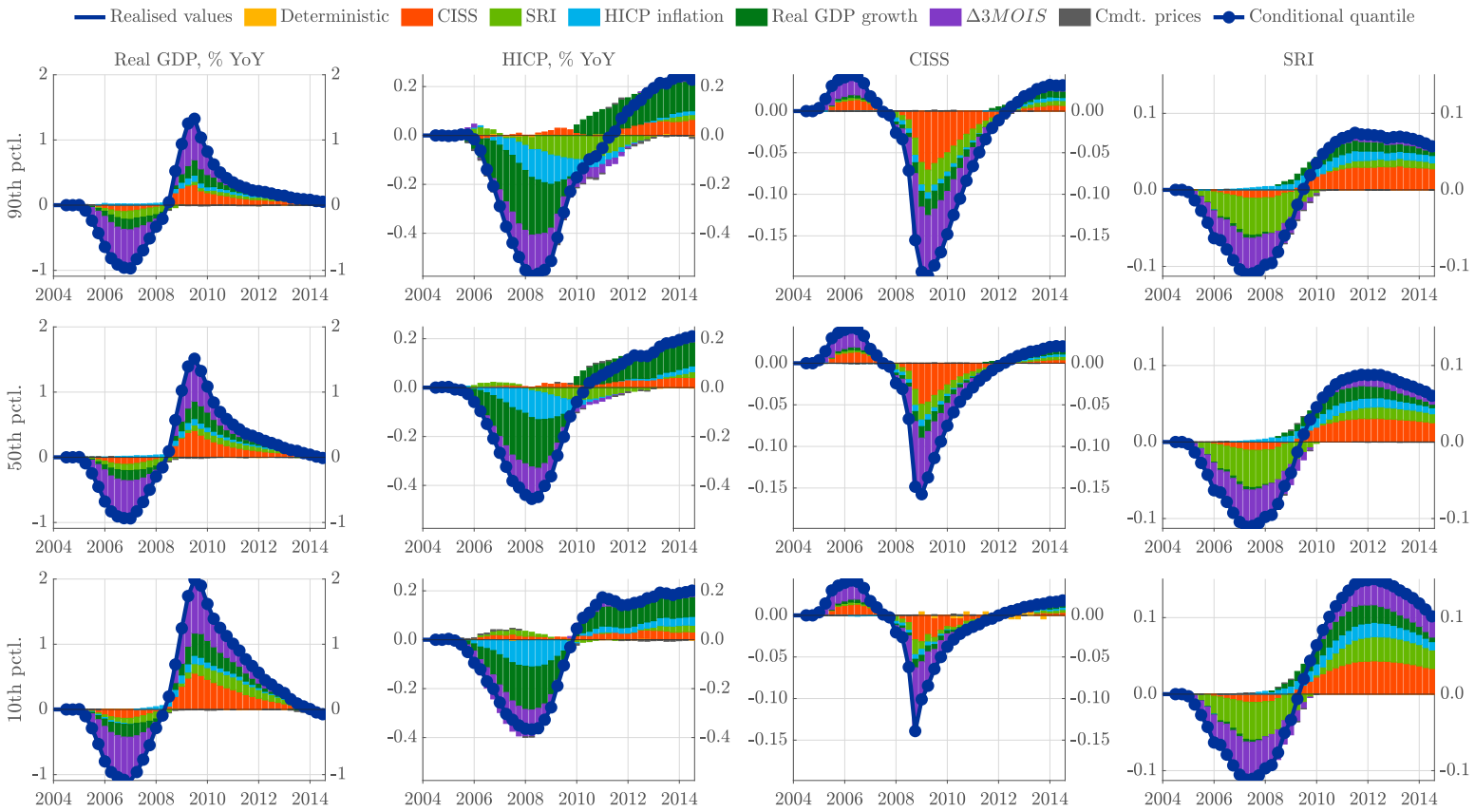

Source: ECB and authors' calculations.
Note: Shapley values are computed for all lags pertaining to a given variable and do not distinguish between each lag for each variable. All $K \cdot 2^{K+M}$ model evaluations are based on 100.000 forward simulations and employ the estimated parameters from the full model specification. Slight differences between the sum of Shapley values and the conditional quantiles can occur due to Monte Carlo error. 'Deterministic' covers constant terms and, to the extent relevant, exogenous shocks and historical values from conversion of quarterly to annual growth rates.

Figure A.9: Shapley value decomposition of select quantiles for endogenous variables in the elevated inflation baseline scenario

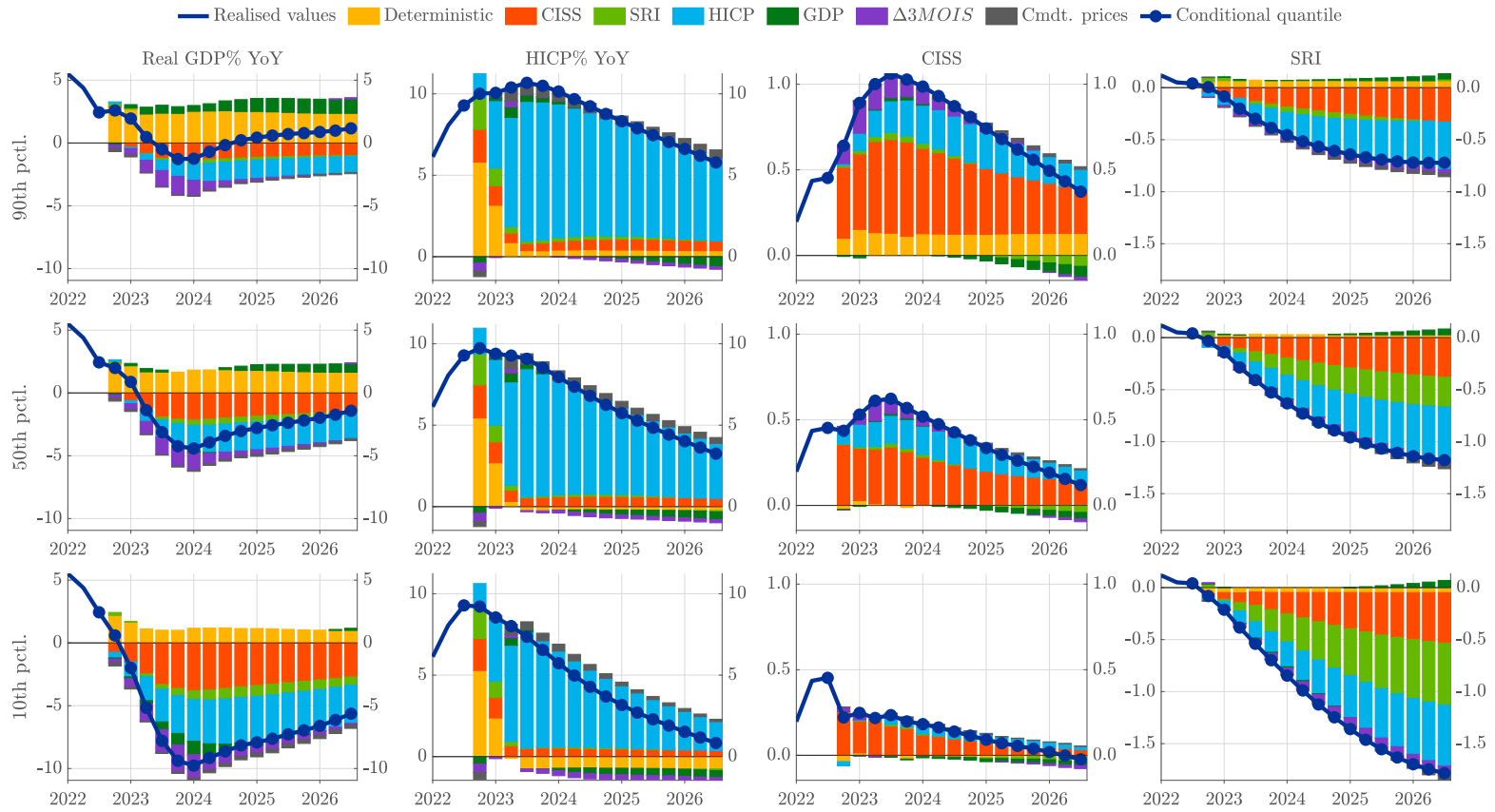

Source: ECB and authors' calculations.
Note: Shapley values are computed for all lags pertaining to a given variable and do not distinguish between each lag for each variable. All $K \cdot 2^{K+M}$ model evaluations are based on 100.000 forward simulations and employ the estimated parameters from the full model specification. Slight differences between the sum of Shapley values and the conditional quantiles can occur due to Monte Carlo error. 'Deterministic' covers constant terms and, to the extent relevant, exogenous shocks and historical values from conversion of quarterly to annual growth rates.

B Forward simulation and scenario analysis using conditional quantiles

This appendix describes in more detail how we apply the QVAR framework for conditional quantile forecasting, both with and without restrictions, the latter of which is the foundation for the scenario analysis performed in this paper.

Central to the forecasting procedure are equations (1) and (2), which we replicate here for convenience,

$$Y_t = C^j D_t + A_0^j Y_t + \sum_{p=1}^{P} A_p^j Y_{t-p} + \sum_{s=0}^{S} B_s^j X_{t-s} + \varepsilon_t^j \tag{B.1}$$

$$F\left(\varepsilon_{i,t}^j < 0 | \Psi_{i,t-1}\right) = j \; \forall \; i = 1, 2, \ldots, K \tag{B.2}$$

B.1 Conditional quantile forecasting

To better understand how the QVAR can be used to simulate the joint conditional distribution forward, it is instructive to consider the univariate version of equation (B.1), dropping exogenous variables without loss of generality, for the one-period-ahead conditional forecast of the jth quantile of variable $i = 1$ at time $\tau + 1$, where τ is the forecast origin

$$y_{1,\tau+1} = C_1^j D_{\tau+1} + \sum_{p=1}^{P} A_{p,1}^j Y_{\tau+1-p} + \varepsilon_{1,\tau+1}^j \tag{B.3}$$

letting subscript i denote the ith row of the relevant matrix and using the fact that A_0^j is lower triangular with a zero diagonal ensuring that $A_{0,1}^j Y_{\tau+1} = 0$. Let $Q_{i,\tau}^j(\cdot)$ denote a quantile operator that produces the jth quantile of a stochastic process conditional on the information set $\Psi_{i,\tau}$ and use it to get the conditional forecast of the jth quantile of $y_{1,\tau+1}$

$$Q_{1,\tau}^j\left(y_{1,\tau+1}\right) = C_1^j D_{\tau+1} + \sum_{p=1}^{P} A_{p,1}^j Y_{\tau+1-p} \tag{B.4}$$

where $Q_{1,\tau}^j\left(\varepsilon_{1,\tau+1}^j\right) = 0$ follows from equation (B.2), while D_{t+1} is deterministic by construction and thus not subject to uncertainty.

More generally, for the endogenous variable, y_i, and any associated quantile forecast, $\lambda_{i,\tau}$, it

similarly follows that $Q_{i,\tau}^{\lambda_{i,\tau+1}}\left(\varepsilon_{i,\tau+1}^{\lambda_{i,\tau+1}}\right)=0$ such that the conditional quantile forecast one period ahead is given by

$$Q_{i,\tau}^{\lambda_{i,\tau+1}}\left(y_{i,\tau+1}\right)=C_{i}^{\lambda_{i,\tau+1}}D_{\tau+1}+\sum_{k=1}^{i-1}A_{0,ik}^{\lambda_{i,\tau+1}}Q_{i,\tau+1}^{\lambda_{i,\tau}}\left(y_{k,\tau+1}\right)+\sum_{p=1}^{P}A_{p,i}^{\lambda_{i,\tau+1}}Y_{\tau+1-p} \tag{B.5}$$

again dropping exogenous variables for convenience and letting matrix subscript ik denote the kth element of the ith row.

Notice that expression (B.5) is still stochastic due to the presence of $y_{1,\tau+1},\ldots,y_{i-1,\tau+1}$ and consequently the set of associated structural shocks $\{\varepsilon_{k,\tau+1}^{\lambda_{k,\tau+1}}\}_{k=1}^{i-1}$ in the first summation, which cannot be conditioned away by the quantile operator for variable i, $Q_{i,\tau}^{\lambda_{i,\tau+1}}(\cdot)$. To circumvent this and allow conditional quantile forecasting, assume that the quantile realisations for each y_k in period $\tau+1$ are given, $\{\lambda_{k,\tau+1}^{*}\}_{k=1}^{K}$, and use the law of iterated quantiles (Chavleishvili and Manganelli (2019)) to sequentially condition away the structural shocks, such that the conditional quantile forecast is purely a function of deterministic terms and lags of endogenous variables

$$Q_{1,\tau}^{\lambda_{1,\tau+1}^{*}}\left(\ldots Q_{i-1,\tau}^{\lambda_{i-1,\tau+1}^{*}}\left(Q_{i,\tau}^{\lambda_{i,\tau+1}^{*}}\left(y_{i,\tau+1}\right)\right)\right)=\overline{\mathbf{C}}_{i,\tau+1}D_{\tau+1}+\sum_{p=1}^{P}\overline{\mathbf{A}}_{p,i,\tau+1}Y_{\tau+1-p} \tag{B.6}$$

where $\overline{\mathbf{C}}_{i,\tau+1}$ and $\overline{\mathbf{A}}_{p,i,\tau+1}$ are nonlinear functions of the relevant matrix coefficients $C^{\lambda_{\iota,\tau+1}^{*}}$ and $A_{\bullet}^{\lambda_{\iota,\tau+1}^{*}}$ in (B.1) for $\iota=1,2,\ldots,i$.

Following Chavleishvili and Manganelli (2019), the procedure can easily be extended to allow for the conditional quantile forecast of any given set of variables at any horizon $h\geq 1$ using the law of iterated quantiles.

As illustrated above, conditional quantile forecasting of up to horizon $H>0$ requires complete quantile paths for $\{Y_{\tau+h}\}_{h=1}^{H}$ and $\{X_{\tau+h}\}_{h=1}^{H}$ to govern the forward dynamics throughout the forecasting period. One immediate way of obtaining the forward paths for quantile realisations is to simply choose them. Deciding on particular quantile paths, however, quickly risks becoming an arbitrary exercise in the context of forward scenario analysis, in which the goal is to project the entire conditional distribution in a unified and agnostic manner.

Alternatively, one may instead consider all possible forward paths for both endogenous and

exogenous variables, of which there are a total of $q^{(K+M)H}$, letting q denote the number of quantiles to be estimated. The conditional quantile forecasts at each horizon are then computed as the empirical quantile over all possible paths. In a medium sized QVAR such as ours, considering all possible paths quickly becomes computationally infeasible for a sufficiently granular set of quantiles.

We consequently opt for the use of simulation methods as in Koenker et al. (2017) and Chavleishvili et al. (2021), who exploit the fact that equations (B.1)-(B.2) implicitly specify the entire conditional forecast distribution of Y, making it possible to directly draw realisations of Y by inverse CDF-sampling.

Repeating the forward simulation enough times to sufficiently explore the probability space, the conditional quantile forecast is then the empirical quantile over all simulations, see also section B.3. The simulation method is an attractive and computationally feasible approach to study the QVAR under different scenarios.

B.2 Scenario analysis in the QVAR

Scenario analysis in the QVAR from the forecast origin τ, H periods ahead, can be implemented in three distinct, though not necessarily mutually exclusive, ways.

i A sequence of structural quantile shocks to one or more endogenous variables, $\{\hat{\epsilon}^{j}_{\tau+h}\}_{h=1}^{H}$.

ii The imposition of fixed paths for the jth quantile of one or more endogenous variables over all or part of the forecast horizon, $\{\hat{y}^{j}_{i,\tau+h}\}_{h=\underline{h_i}}^{\overline{H_i}}$, letting $\underline{h_i}$ and $\overline{H_i}$ denote the start and end point for variable i's fixed path.

iii Choosing a quantile path and consequently the estimation coefficients governing the dynamic properties of one or more endogenous variables, $\{\hat{j}_{i,\tau+h}\}_{h=\underline{h_i}}^{\overline{H_i}}$, where $j_{i,\tau+h}$ is the quantile realisation of variable i at time $\tau+h$ as per equation (B.1).

While the methods above are described for endogenous variables, all of them naturally extend to exogenous variables. We describe each in more detail below.

B.2.1 Method i: Structural shocks

Much like the linear VAR, method i imposes a sequence of structural shocks, $\{\hat{\epsilon}^{j}_{\tau+h}\}_{h=1}^{H}$, on select system variables. Unlike the linear VAR, where structural shocks shift the location of the

conditional distribution, the QVAR in principle allows for individual points on the conditional distribution to be hit by separate shocks. Consider, for instance, the case where the model is estimated for three quantiles, e.g. $j \in \{0.1, 0.5, 0.9\}$. Then it would be possible to model a shift in the right tail of the distribution by designing a sequence of shocks where $\hat{\epsilon}^{0.1}_{i,\tau+h} = \epsilon^{0.5}_{i,\tau+h} = 0$ and $\hat{\epsilon}^{0.9}_{i,\tau+h} \neq 0$. In practice, asymmetric structural shocks should be implemented with caution, as it can easily result in quantile crossing (Bassett Jr and Koenker (1982)), whereby the choice of $\hat{\epsilon}^{0.9}_{i,\tau+h}$ in the above example can imply that $Q^{0.9}_{i,\tau}(y_{i,\tau+h}) < Q^{0.5}_{i,\tau}(y_{i,\tau+h})$. For this reason, structural shocks implying changes in higher order moments of the conditional distribution may require additional assumptions about the interactions between quantile shocks or the use of techniques to handle quantile crossing specifically, e.g. Chernozhukov et al. (2010). For our purposes, it suffices to consider only location shifts in the conditional distribution by imposing $\hat{\epsilon}^{j}_{i,\tau+h} = \hat{\epsilon}_{i,\tau+h} \, \forall \, j$ rather than changes in higher order moments (see e.g. Schüler (2020) for an example of asymmetrical quantile shock implementation).

B.2.2 Method ii: Fixed paths

This is the quantile equivalent of forecasting conditional on a variable following a specific path (see e.g. Waggoner and Zha (1999), Leeper and Zha (2003) and Giannone et al. (2019)). Using the random coefficient representation of the QVAR, imposing a fixed path on the jth quantile of variable i at time $\tau + h$, $\hat{y}^{j}_{i,\tau+h}$, implies a sequence of structural shocks, $\{\epsilon_{\tau+h}(U_{\tau+h})\}_{h=\underline{h}}^{\overline{H}}$, which ensures that the restrictions are satisfied. As above, adding shocks to individual quantiles necessarily requires consideration of potential quantile crossing. Even when no quantile crossing occurs, however, a further complication arises from the fact that multiple sets of structural shocks across the system variables are likely to satisfy the restrictions. In the linear VAR, this issue is often solved by minimising a criterion function with respect to the sequence of shocks conditional on the restrictions, e.g. Doan et al. (1984) and Clarida and Coyle (1984). However, in the QVAR context with multiple potential restrictions on specific quantiles, identifying the optimal set of shocks can quickly become intractable. To the best of our knowledge, we are not aware of any examples in the literature of imposing restrictions on multiple quantiles in a QVAR system, leaving it as a potential topic of future research.

We take two simplifying approaches to fixed paths in our applications. In one, we assume a collapse of the conditional forecast distribution to the conditioning path, that is, $\hat{y}^{j}_{i,\tau+h} = \hat{y}_{i,\tau+h} \, \forall \, j$ and that this is ensured by a set of potentially asymmetric shocks hitting only the

quantiles of the restricted variables in the relevant periods. In a second, less restrictive approach, we only require that the means of the conditional forecast distribution satisfy the restrictions. To impose this, note that the conditional expectation of the QVAR in its random coefficient form, leaving out deterministic terms and exogenous variables without loss of generality, can be written as

$$\begin{aligned}\mathbb{E}_{\tau+h-1}\left[Y_{\tau+h}\right] &= \mathbb{E}_{\tau+h-1}\left[A_0\left(U_{\tau+h}\right)Y_{\tau+h}\right] + \sum_{p=1}^{P}\mathbb{E}_{\tau+h-1}\left[A_p\left(U_{\tau+h}\right)Y_{\tau+h-p}\right] + \mathbb{E}_{\tau+h-1}\left[\epsilon^j_{\tau+h}\right] \\ &= \left(I_K - \check{A}_0\right)^{-1}\left(\sum_{p=1}^{P}\check{A}_p Y_{\tau+h-p} + \epsilon^*_{\tau+h}\right)\end{aligned} \tag{B.7}$$

where $\check{A}_\bullet = \mathbb{E}_{\tau+h-1}\left[A_\bullet\left(U_{\tau+h}\right)\right]$, $\epsilon^*_{\tau+h} = \mathbb{E}_{\tau+h-1}\left[\epsilon^j_{\tau+h}\right]$ and we have used that $U_{\tau+h}$ is i.i.d. For a sufficiently granular set of estimated quantiles, η, (B.7) allows us to approach the mean QVAR prediction as a linear VAR using the average of estimated quantile coefficients. Further, we can use standard methods to identify the sequence of structural shocks to the mean, $\{\check{\epsilon}_{\tau+h}\}_{h=1}^{H}$, that satisfy the restrictions, in our case by minimising the sum of squared shocks. Additionally, this approach combined with the structural nature of the QVAR permits the inclusion of prior information about which specific shocks are driving the conditional forecasts akin to Antolin-Diaz et al. (2021). For instance, one could impose that a particular outcome for expected growth is entirely explained by macrofinancial shocks.

A particular caveat of scenario analysis using method ii is that the structural shocks implied by a given path can lead to strange behaviour in the unrestricted variables if they are sufficiently inconsistent with the QVAR dynamics. A second consideration is whether the given path represents a sufficiently likely scenario within the estimated model. Indeed, for the case of monetary policy paths in a linear VAR, Leeper and Zha (2003) make the distinction between moderate and immodest policy interventions, where the latter implies a sequence of shocks so far removed from the intrinsic model dynamics, that one should consider whether it expresses a structural break not properly captured by the conditional forecasting model. As such, caution should be used when implementing method ii.

B.2.3 Method iii: Quantile paths

Finally, method iii takes advantage of the QVAR structure by restricting the point on the conditional forecast distribution which the individual variables realise in specific periods. Put differently, the set of coefficients that are drawn from when simulating the model forward in an unrestricted environment, $\{C(U_{\tau+h}), A_\bullet(U_{\tau+h}), B_\bullet(U_{\tau+h})\}$, is reduced to a subset for the restricted variables in the desired periods containing only the coefficients pertaining to a single quantile. Recalling the random coefficient representation of the QVAR, restrictions on the quantile path then implies choosing a sequence of points on the interval $(0;1)$, $\{\hat{U}_{\tau+h}\}_{h=\underline{h}}^{\overline{H}}$ for one or more variables and periods, such that the conditional forecast is given by

$$Y_{\tau+h} = C\left(\hat{U}_{\tau+h}\right) D_{\tau+h} + \sum_{p=0}^{P} A_p\left(\hat{U}_{\tau+h}\right) Y_{\tau+h-p} + \sum_{s=0}^{S} B_s\left(\hat{U}_{\tau+h}\right) X_{\tau+h-s} \tag{B.8}$$

Doing scenario analysis with method iii in turn implies that fixing the realised point on the conditional distribution, unlike method ii, still leaves the variable in question, and consequently its conditional forecast distribution, endogenous and responsive to prior system developments. This type of semi-endogenous restriction can be an attractive feature in scenario analysis, in which one wishes to push certain variables along a given path but still leave them susceptible to counterfactual movements in other variables, e.g. policy variables.

B.3 Algorithm to simulate the QVAR forward

To obtain forecasts of conditional quantiles of our system of interest, Y, we follow the simulation algorithm given by Chavleishvili et al. (2021).

Specifically, let H denote the forecast horizon, τ the forecast origin, N the number of simulations and η a sufficiently large set of q quantiles between 0 and 1 symmetric around the median. For our purposes we let $\eta = \{0.05, 0.10, \ldots, 0.90, 0.95\}$ in order to thoroughly explore the probability space. It is important that N is large such that a sufficient number of different paths are explored and consequently reflected in any derived statistics. Unless otherwise stated, we set $N = 10^6$.

We then proceed as follows.

1. For all endogenous variables and all $j \in \eta$, obtain estimates of the quantile coefficients in

(B.1) as well as for each exogenous variable in X using the univariate version of (B.1)

$$x_{m,t} = C_m^{X,j} D_t + \sum_{s=1}^{S} A_{m,s}^{X,j} x_{m,t-s} + \varepsilon_{m,t}^{X,j} \tag{B.9}$$

$$F\left(\varepsilon_{m,t}^{X,j} < 0 | \Psi_{m,t}^{X}\right) = j \tag{B.10}$$

for $m = 1, \ldots, M$.

2. Set $n = 1$.

   2.1. Set $h = 1$.

      2.1.1. Select $K + M$ random numbers, κ, from the uniform distribution $U(0, 1)$ and select the corresponding quantiles in η based on proximity.

      2.1.2. If any quantile paths, $\hat{U}_{\tau+h}$, have been imposed, cf. restriction method B.2.3, replace the randomly selected quantiles in κ from the previous step with $\hat{U}_{\tau+h}$ for the relevant variables.

      2.1.3. Stack the variable specific rows from the matrices of quantile coefficients corresponding to the elements in κ, such that

$$\tilde{C}^{\tau+h} = \begin{bmatrix} C_1^{\kappa_1} \\ \vdots \\ C_i^{\kappa_i} \\ \vdots \\ C_K^{\kappa_K} \end{bmatrix}, \qquad \tilde{A}_p^{\tau+h} = \begin{bmatrix} A_{p,1}^{\kappa_1} \\ \vdots \\ A_{p,i}^{\kappa_i} \\ \vdots \\ A_{p,K}^{\kappa_K} \end{bmatrix}, \qquad \tilde{B}_s^{\tau+h} = \begin{bmatrix} B_{s,1}^{\kappa_1} \\ \vdots \\ B_{s,i}^{\kappa_i} \\ \vdots \\ B_{s,K}^{\kappa_K} \end{bmatrix}$$

      for $p = 0, \ldots, P$ and $s = 0, \ldots, S$, and letting $A_{p,i}^{j}$ denote the i'th row of A_p^j and so forth. Similarly for all exogenous variables, set $\tilde{C}_m^{X,\tau+h} = C_m^{X,\kappa_{K+m}}$ and $\tilde{A}_{m,s}^{X,\tau+h} = A_{m,s}^{X,\kappa_{K+m}}$.

      2.1.4. Compute the conditional forecast of each of the m variables in $X_{\tau+h}^{(n)}$ using (B.9) and the relevant quantile coefficients determined in step 2.1.3 as

$$x_{m,\tau+h}^{(n)} = \tilde{C}_m^{X,\tau+h} D_{\tau+h} + \sum_{s=1}^{S} \tilde{A}_{m,s}^{X,\tau+h} x_{m,\tau-s}^{(n)} + \hat{\epsilon}_{m,\tau+h}^{X,j} \tag{B.11}$$

where $\hat{\epsilon}^{X,j}_{m,\tau+h}$ is a shock ensuring that any restrictions using either methods B.2.1 or B.2.2 are satisfied.

2.1.5. Compute the conditional forecast of $Y^{(n)}_{\tau+h}$ using (1) and the relevant quantile coefficients determined in step 2.1.3 as

$$Y^{(n)}_{\tau+h} = \left(I - \tilde{A}^{\tau+h}_0\right)^{-1} \left(\tilde{C}^{\tau+h} D_{\tau+h} + \sum_{p=1}^{P} \tilde{A}^{\tau+h}_p Y^{(n)}_{\tau+h-p} + \sum_{s=0}^{S} \tilde{B}^{\tau+h}_s X^{(n)}_{\tau+h-s} + \hat{\epsilon}_{\tau+h}\right) \tag{B.12}$$

where $\hat{\epsilon}_{\tau+h}$ is a $K \times 1$ vector of shocks ensuring that any restrictions using either methods B.2.1 or B.2.2 are satisfied.

2.1.6. If $h < H$, set $h = h + 1$ and return to step 2.1.1

2.2. If $n < N$, set $n = n + 1$ and return to step 2.1.

3. Let $\check{\mathbf{Y}}_{\tau+h} = \{Y^{(n)}_{\tau+h}\}^{N}_{n=1}$ be the set of N simulated forecasts of $Y_{\tau+h}$ and compute the ω'th conditional quantile forecast of $y_{i,\tau+h}$ as

$$Q^{\omega}_{i,\tau+h}\left(y_{i,\tau+h}\right) = Q^{\omega}\left(\check{\mathbf{y}}_{i,\tau+h}\right) \tag{B.13}$$

recalling $Q^{\omega}_{i,\tau}(\cdot)$ as the ω'th quantile function conditional on the information set, $\Psi_{i,\tau-1}$, and letting $Q^{\omega}(\cdot)$ denote the empirical quantile function. Note that ω isn't restricted to lie in η and can be anywhere in the interval $(0; 1)$.

The algorithm above can be used to compute any statistic based on conditional forecast quantile forecasts of Y.

Following an approach similar to the general case of Koop et al. (1996) and the QVAR specific case of Chavleishvili and Mönch (2023), we compute generalised quantile impulse responses, G-QIRFs, for any $K \times 1$ vector of structural shocks arriving at time $\tau + h^*$, $\nu_{\tau+h^*}$, by obtaining a separate set of simulations, $\check{\mathbf{Y}}^{*}_{\tau+h} = \{Y^{(n)}_{\tau+h} | \nu_{\tau+h^*}\}^{N}_{n=1}$, where we condition on the shock. The generalised quantile impulse response function, $g^{\omega}_{i,\tau+h}\left(\nu_{\tau+h^*}\right)$ then follows as

$$g^{\omega}_{i,\tau+h}\left(\nu_{\tau+h^*}\right) = Q^{\omega}\left(\check{\mathbf{y}}^{*}_{i,\tau+h}\right) - Q^{\omega}\left(\check{\mathbf{y}}_{i,\tau+h}\right) \tag{B.14}$$

C Shapley value computation in the QVAR

The nonlinear property of the QVAR, while attractive in terms of analysing the conditional distribution of a system of variables, adds a layer of complexity when attempting to apply standard methods for linear VARs, for instance forecast error variance decomposition and historical decompositions. To see this consider the simple structural VAR(1) model

$$Y_t = D + \Phi Y_{t-1} + \Omega^{-1}\varepsilon_t \tag{C.1}$$

where Ω contains the contemporaneous interaction between the endogenous variables, D and Φ consist of reduced form parameters, while ε are the K structural shocks. Recasting (C.1) in the moving average-representation we get

$$Y_t = (I - \Phi)^{-1} D + \sum_{\tau=0}^{\infty} \Phi^{\tau}\Omega^{-1}\varepsilon_{t-\tau} \tag{C.2}$$

from which it becomes clear that Y can be decomposed into contributions from the individually identified structural shocks over the entire sample, since all relevant parameters and shocks in (C.2) have been estimated. In a similar manner, the contribution of structural shock, i, to the forecast error variance for variable j at horizon h can be expressed as in Lütkepohl (1990) by

$$\omega_{j,i,h} = \sum_{\iota=0}^{h-1} \left(e_j^{'}\Phi^{\iota}\Omega e_i\right)^2 \tag{C.3}$$

where e_k is the k'th column in I_K. As can be seen, both the historical decomposition and the forecast error variance decomposition derived from (C.2) and (C.3), respectively, can be readily obtained as soon as the SVAR has been estimated and identified. In the case of the QVAR, however, the parameters governing the system dynamics change randomly in each period, thus making the formulas in (C.2) and (C.3) insufficient without directly assuming the quantile paths travelled by the endogenous variables over all periods.

Shapley values, as discussed in Lundberg and Lee (2017), are an additive feature attribution method, meaning that a prediction generated by the model, $m(\mathcal{F})$, with the set of model features, $\mathcal{F}$, as inputs can be written as

$$m(\mathcal{F}) = s_0 + \sum_{f \in \mathcal{F}} s_f \mathcal{M}(f) \tag{C.4}$$

where $\mathcal{M}(f)$ is a function returning the value 1 if the feature f is included in the model and 0 otherwise, s_f is the Shapley value associated with model feature f, and s_0 is the Shapley value associated with an empty model, i.e. $f(\emptyset)$. The Shapley value, s_f, is then given by

$$s_f = \sum_{\mathcal{G} \subseteq \mathcal{F} \setminus f} \frac{1}{(|\mathcal{G}| + 1) \binom{|\mathcal{F}|}{|\mathcal{G}|+1}} \left(m_{\mathcal{G} \cup f}(\mathcal{G} \cup f) - m_{\mathcal{G}}(\mathcal{G}) \right) \tag{C.5}$$

letting $|\mathcal{H}|$ denote the number of elements in the set, $\mathcal{H}$, and $m_{\mathcal{H}}$ the model generating the prediction and trained on the input variables in $\mathcal{H}$.

Equation (C.5) is essentially a weighted average of all possible contributions to the model predictions generated by including the feature of interest, f, in all model permutations excluding it , $\mathcal{G}$. Note that for all $\mathcal{G}$, the model m is retrained, or re-estimated, thereby requiring estimating a total of $2^{|\mathcal{F}|}$ models to obtain all $|\mathcal{F}| + 1$ Shapley values, including s_0. By extension, Shapley values are agnostic to the underlying model, since they only consider the predictions generated by the different permutations. For this reason, methods based on Shapley values are often used in the machine learning literature to approximate how different model inputs contribute to a given model prediction, even if the model is highly nonlinear. For the same reason, Shapley values are a natural candidate to study the drivers of conditional forecast quantiles generated by the QVAR.

Recalling the QVAR in equation (1), we let the K endogenous variables in Y and the M exogenous variables in X be the set of considered model features, $\mathcal{F}^Q$, and let the empty model contain only the deterministic terms in D. Depending on the desired degree of granularity, one may want to consider each lag for each endogenous and exogenous variable as its own model feature, although for our purposes, we simply consider all contemporaneous and lagged values of a given variable as representing one model feature, yielding a total of $K + M$ features. Let then $q^j_{i,\tau+h}\left(\mathcal{F}^Q\right)$ be the h-period ahead prediction of variable i's j'th quantile with forecast origin τ based on the model features in $\mathcal{F}^Q$ as inputs. We can then decompose the quantile projection according to (C.4), such that

$$q^j_{i,\tau+h}\left(\mathcal{F}^Q\right) = s^j_{0,i,\tau+h} + \sum_{f \in \mathcal{F}^Q} s^j_{f,i,\tau+h} \mathcal{M}^Q(f) \tag{C.6}$$

where $\mathcal{M}^Q$ is a QVAR-specific version of the related function in equation (C.4) and s the corresponding Shapley values. Notice that the Shapley values are computed for all quantiles,

$j \in \kappa$, for each endogenous variable, $i = 1, \ldots, K$, at each forecast horizon, $h = 1, \ldots, H$. For large models, this level of granularity would typically present a steep increase in computational complexity and require approximation based methods to obtain the Shapley values, however, given the relatively parsimonious parameterisation of our QVAR, we instead opt to compute them directly with equation (C.5).

As mentioned above, getting the Shapley values requires re-estimating the model while permuting over the $K+M$ features in the case of the QVAR. Removing and reintroducing variables in the estimation can, however, lead to endogeneity issues known from standard regression analysis. To the extent that the omission of a feature yields biased parameter estimates for the remaining model features, and consequently a different quantile projection, the resulting Shapley values will tend to assign explanatory power to the omitted feature, even if it has none in the full model specification.

For this reason, we compute Shapley values using the full model parameter estimates for all permutations, which in terms of equation (C.5) amounts to the modified formula

$$s^j_{f,i,\tau+h} = \sum_{\mathcal{G} \subseteq \mathcal{F}^Q \setminus f} \frac{1}{(|\mathcal{G}|+1)\binom{|\mathcal{F}^Q|}{|\mathcal{G}|+1}} \left(q^j_{\mathcal{F}^Q,i,\tau+h}(\mathcal{G} \cup f) - q^j_{\mathcal{F}^Q,i,\tau+h}(\mathcal{G}) \right) \tag{C.7}$$

An important distinction when assessing Shapley values is between explainability and interpretability. The former can be viewed as equivalent to a positive statement, in that it provides information on how important a model feature is to a given prediction. Interpretability, on the other hand, is a statement about causation. Because Shapley values are agnostic to the underlying model, and in particular the identified structure of the SVAR, one should be careful to not conflate them with information about how structurally identified shocks are driving the system, as one may otherwise do in the linear SVAR.

Acknowledgements

We thank Simone Manganelli and Massimiliano Marcellino for useful comments and suggestions.

Sulkhan Chavleishvili
Aarhus University, Aarhus, Denmark; email: sulkhan.chavleishvili@econ.au.dk

Manfred Kremer
European Central Bank, Frankfurt am Main, Germany; email: Manfred.Kremer@ecb.europa.eu

Frederik Lund-Thomsen
European Central Bank, Frankfurt am Main, Germany; email: Frederik_Ole.Lund-Thomsen@ecb.europa.eu

Postal address 60640 Frankfurt am Main, Germany
Telephone +49 69 1344 0
Website www.ecb.europa.eu

PDF ISBN 978-92-899-6118-9 ISSN 1725-2806 doi:10.2866/197182 QB-AR-23-070-EN-N